Table II. Primer sequences used in RT-PCR analyses in human cancer cell lines.

Gene	Sense	Antisense
DKFZP564O0823	5'-CCATCTGGACTAGCTCTCCACA-3'	5'-GTGCTGGTCACAGTGGAGCTA-3'
ADAMTS4	5'-GTGGAGTCTCCACTTGCGACA-3'	5'-CCAGGGCGAGTGTTTGGTCT-3'
DNER	5'-GTGGTGAAGGTCAGCACCTGT-3'	5'-GGCTGAGGGCACAGAAGTCAA-3'
NGFR	5'-GTTCTCCTGCCAGGACAAGCA-3'	5'-GTCCACGGAGATGCCACTGT-3'
LRRN6A	5'-GTACAACCTCAAGTCACTGGAGGT-3'	5'-CATTGAGCACCGCGCAGGTAGTT-3'
ECSM2	5'-CAATGACCCAGACCTCTAGCTCT-3'	5'-GCAGCTTTCAGACAGCCCTGA-3'
LGALS3BP	5'-CCCACAGACCTGCTCCAACT-3'	5'-CCGTCTGGACTGATAGACCAGTT-3'
PTPRF	5'-CAGCCCCTACTCGGATGAGAT-3'	5'-GCGATGACATTCGCATAGCGGTT-3'
FCGRT	5'-CTCTCCCTCCTGTACCACCTT-3'	5'-GTGCCCTGCTTGAGGTCGAAAT-3'
LAMP2	5'-GTGCAGTTCGGACCTGGCTT-3'	5'-CAGCTGCCTGTGGAGTGAGTT-3'
RCN1	5'-GACAATGATGGGGATGGCTTTGTCA-3'	5'-CGGAATTCGTTAAACTGCTCCCGTT-3'
MMP14	5'-CAACATTGGAGGAGACACCCACTTT-3'	5'-GTTCCAGGGACGCCTCATCAAA-3'
SDC2	5'-GCTCCATTGAAGAAGCTTCAGGAGT-3'	5'-GCCTTCTGATAAGCAGCACTGGAT-3'
DAG1	5'-CGGAGGCAGATCCATGCTACA-3'	5'-GGCAGTTTCCAATCTGGTGATGGA-3'
EPCR	5'-CTACTTCCGCGACCCCCTATCA-3'	5'-GCGAAGTGTAGGAGCGGCTT-3'
CD97	5'-CAAGACAAGCTCAGCCGAGGT-3'	5'-CTCCCCCATCGGAGGACTCAA-3'
CD99L2	5'-CAAGAAACCCAGTGCTGGGGAT-3'	5'-GTACGCTGAACAGCTGGCTCT-3'
IGFBP5	5'-CTCAACGAAAAGAGCTACCGCGA-3'	5'-CTGTCGAAGGTGTGGCACTGAA-3'
CLU	5'-CAATGAGACCATGATGGCCCTCT-3'	5'-CCGGGCTATGGAAGTGGATGT-3'
LSAMP	5'-GGACAACATCACCGTGAGGCA-3'	5'-GGAGACCTCGTTGGCAGCTT-3'
NPTN	5'-CCCTGTCACCCTGCAGTGTA-3'	5'-CCAATGGCGTTGGTGGCATTACA-3'
EFNA5	5'-CCAGAGGGGTGACTACCATATTGA-3'	5'-CGGCTGACTCATGTACGGTGT-3'
PODXL	5'-CTCCACAGCCACAGCTAAACCTA-3'	5'-CTGGCAGGGTAGGTGTTCTCAA-3'
TMEM123	5'-CCATGGCGGCATCTGCAAACAT-3'	5'-CGATACCGAATGCCTCTTCTTGAGT-3'
PCOLCE	5'-CGGACGCTTTTGTGGGACCTT-3'	5'-GGCAGCTTGACTTTAGGCTCAGTT-3'
SEZ6L2	5'-GCACCTGCACTTTGAAAGGGTCT-3'	5'-GTCCCCTTCCCGCACATTCAATAT-3'
IGFBP4	5'-GAAGCCCCTGCACACACTGAT-3'	5'-GAAAGCTGTCAGCCAGCTGGT-3'
IGFBP3	5'-GCATCTACACCGAGCGCTGT-3'	5'-GGGACTCAGCACATTGAGGAACTT-3'
LOX	5'-GTCACTGGTTCCAAGCTGGCTA-3'	5'-GGAATATCTTGGTCGGCTGGGTA-3'
CTGF	5'-GCGTGTGCACCGCCAAAGAT-3'	5'-CGGTATGTCTTCATGCTGGTGCA-3'
SPARC	5'-CTGCCAGAACCACCACTGCAA-3'	5'-CTGCCAGTGTACAGGGAAGATGT-3'
QSCN6	5'-GGCTGACCTGGAATCTGCACT-3'	5'-CATTGTGGCAGGCAGAACAAAGTTC-3'
EDIL3	5'-CTGTGAGTGCCCAGGCGAATTTA-3'	5'-GATTTCATACCCAGAGGCTCAGAACA-3'
MXRA8	5'-GTACACCTGCAACCTGCACCAT-3'	5'-GGGACGATGACATTGATGACGTTGT-3'
PRRT3	5'-GCTGACAGTCACAGGAACTCTGA-3'	5'-GCCTCCTGCAAGTGTTCCTCAA-3'
LRP1	5'-CAATGGCCTGACGCTGGACTAT-3'	5'-CGGTGTCACACTTCCACCAGA-3'
ISLR	5'-GCTCCGCTGCAACTCAACCACAA-3'	5'-CTCAGCACTGCCCAGCTCATT-3'
COL6A1	5'-GCAGTACAGCCACAGCCAGAT-3'	5'-GTCAAAGTTGTGGCTGCCCAC-3'
TIMP1	5'-GACCTCGTCATCAGGGCCAA-3'	5'-GCAAGGTGACGGGACTGGAA-3'
LAMP1	5'-CACGTTACAGCGTCCAGCTCAT-3'	5'-CCTTGTAGGAAAAACCGGCTAGAAC-3'
SERPINH1	5'-CTGCTGCGCTCACTCAGCAA-3'	5'-CGTGATGGGGCATGAGGATGAT-3'
COL1A1	5'-CACCTCAAGAGAAGGCTCACGAT-3'	5'-CCACGCTGTTCTTGCAGTGGTA-3'
GAPDH	5'-ACCACAGTCCATGCCATCAC-3'	5'-TCCACCACCCTGTTGCTGTA-3'

The RNA sequences used are as follows: siEF1 (sense 5'-GGC AGCAGAACCCUUCUUAdCdG-3', antisense 5'-UAAGA AGGGUUCUGCUGCCdCdG-3'). SJES-5 cells were plated on a 6-well plate and propagated in RPMI-1640 medium supplemented with 10% FBS. Twenty-four hours later, for transfection, 1 μl of 10 pmol siRNA was diluted with 99 μl of Opti-MEM (Invitrogen), and 2 μl of siFECTOR reagent (B-Bridge International, Mountain View, CA, USA) was diluted with 98 μl of Opti-MEM. Both solutions were mixed gently and incubated at room temperature for 5 min. The mixture was diluted with 800 μl of Opti-MEM, and left at room temperature for 15 min. Next, 1 ml of RNA/liposome

Table III. Genes isolated by the retrovirus-mediated signal sequence trap method (SST-REX).

Isolated gene	Accession number[a]	Frequency[b]
Granulin (GRN)	NM_002087	22
Alzheimer disease amyloid ß A4 precursor protein	NM_201414	16
Procollagen-proline, 2-oxoglutarate 4-dioxygenase	NM_000918	14
NODAL modulator 2 (NOMO2)	NM_173614	12
NODAL modulator 1 (NOMO1)	NM_014287	12
NODAL modulator 3 (NOMO3)	NM_001004067	11
Golgi apparatus protein 1 (GLG1)	NM_012201	10
Podocalyxin-like (PODXL)	NM_001018111	6
Lysosomal-associated membrane protein 2 (LAMP2)	NM_013995	6
Insulin-like growth factor binding protein 3 (IGFBP3)	NM_000598	6
Basigin	NM_198589	6
Dystroglycan 1	NM_004393	6
DKFZP564O0823 protein	NM_015393	5
Ephrin-A5	NM_001962	4
SPARC	NM_003118	4
CD97	NM_001025160	4
Calreticulin	NM_004343	4
Insulin-like growth factor binding protein 4 (IGFBP4)	NM_001552	4
Poliovirus receptor	NM_006505	3
Syndecan 2	NM_002998	3
Seizure-related 6 homolog like 2	NM_201575	3
CD276	NM_025240	3
TMED7	NM_181836	3
Ribophorin II	NM_002951	3
Niemann-Pick disease, type C1	NM_000271	3
TMEM165	NM_018475	3
MHC class I antigen	NM_005514	3
Colony stimulating factor 2	NM_000758	3
NGFR	NM_002507	2
Ribophorin I	NM_002950	2
Proline-rich transmembrane protein 3	NM_207351	2
Custerin	NM_203339	2
Prosaposin	NM_002778	2
Leucine rich repeat neuronal 6A (LRRN6A)	NM_032808	2
Lysosomal-associated membrane protein 1 (LAMP1)	NM_005561	2
Quiescin Q6	NM_001004128	2
Neuroplastin	NM_017455	2
Reticulocalbin 1	NM_002901	2
Hemicentin 1	NM_031935	2
Matrix metallopeptidase 14 (MMP14)	NM_004995	2
Collagen, type VI, α1	NM_001848	2
MHC class I polypeptide-related sequence A	NM_000247	2
Low density lipoprotein-related protein 1 (LRP1)	NM_002332	2
TMEM123	NM_052932	2
Collagen, type XV, α1	NM_001855	2
Protein kinase C substrate 80K-H	NM_002743	2
EGF-like module containing, mucin-like, hormonereceptor-like 2	NM_152920	2
Collagen, type I, α2	NM_000089	2
Lectin, galactoside-binding, soluble, 3 bindingprotein	NM_005567	2
Collagen, type VII, α1	NM_000094	2

Table III. Continued.

Isolated gene	Accession number[a]	Frequency[b]
Protein tyrosine phosphatase, receptor type, F	NM_130440	1
Connective tissue growth factor	NM_001901	1
Protein disulfide isomerase family A, member 4	NM_004911	1
Immunoglobulin superfamily containing leucine-richrepeat (ISLR)	NM_005545	1
Collagen, type I, α1	NM_000088	1
Procollagen C-endopeptidase enhancer (PCOLCE)	NM_002593	1
Chromosome 1 open reading frame 56	NM_017860	1
TIMP metallopeptidase inhibitor 1 (TIMP1)	NM_003254	1
Insulin-like growth factor binding protein 5 (IGFBP5)	NM_000599	1
Solute carrier family 24 member 6 (SLC24A6)	NM_024959	1
Neural cell adhesion molecule 2 (NCAM2)	NM_004540	1
Collagen, type V, α1	NM_000093	1
CD248	NM_020404	1
Fc fragment of IgG, receptor, transporter, α	NM_004107	1
Nucleobindin 1	NM_006184	1
δ-notch-like EGF repeat-containing transmembrane (DNER)	NM_139072	1
Limbic system-associated membrane protein (LSAMP)	NM_002338	1
Lysyl oxidase (LOX)	NM_002317	1
Endothelial cell-specific molecule 2 (ECSM2)	NM_001077693	1
Isolate Tor36 (ZE657) mitochondrion	AY738975	1
Lectin, mannose-binding, 1	NM_005570	1
CD99 molecule-like 2	NM_031462	1
EGF-like repeats and discoidin I-like domains 3	NM_005711	1
SIL1 homolog, endoplasmic reticulum chaperone	NM_022464	1
ADAM with thrombospondin type 1 motif, 4 (ADAMTS4)	NM_005099	1
Matrix-remodelling associated 8 (MXRA8)	NM_032348	1
Protein C receptor, endothelial	NM_006404	1
Tissue factor pathway inhibitor	NM_001032281	1
Serpin peptidase inhibitor, clade H member 1 (SERPINH1)	NM_001235	1
Protocadherin γ subfamily A.6	NM_032086	1

[a]Accession number in GenBank protein database. [b]Number of the clones isolated by SST-REX.

complex was added to 1 ml of OPTI-MEM supplemented with 20% FBS. Then, the culture medium of the SJES-5 cells was replaced with the 2 ml of the RNA/liposome-containing medium prepared. Twenty-four hours after transfection, culture medium was replaced with the 2 ml of Opti-MEM with 10% FBS, and grown for another 48 h. The cells were harvested and then total RNA was extracted for RT-PCR analysis. The primers used for RT-PCR are as follows: EWS-FLI1-S, 5'-GGGTATGGCACTGGTGCTTATGAT-3'; EWS-FLI1-AS, 5'-GGCTCCAAAGAAGCTGGAGGAA-3'; EWS-S, 5'-GCCCAGCCCACTCAAGGATAT-3'; EWS-AS, 5'-CCCCTGTGCTAGATTGAGGTTGA-3'; FLI1-S, 5'-GCCAACGCCAGCTGTATCA-3'; FLI1-AS, 5'-GTGTGAAGGCACGTGGGTGTT-3'.

IP-Western analysis. IP-Western blot analysis was performed as previously described (39) with some modifications. Briefly, cells were lysed in RIPA buffer [50 mM Tris-HCl (pH 7.4), 150 mM NaCl, 1% NP40, 0.5% deoxycholate, 0.1% SDS]. Cell lysates were immunoprecipitated with the rabbit polyclonal anti-ADAMTS4 antibody. SDS-polyacrylamide gel electrophoresis was performed under reducing conditions using 5-20% gradient gel (Wako Pure Chemical Industries, Osaka, Japan). After transfer to a nitrocellulose membrane, the blot was probed with the rabbit polyclonal anti-ADAMTS4 antibody and then with the HRP-conjugated goat anti-rabbit IgG secondary antibody. ADAMTS4 protein was detected with enhanced chemiluminescence (ECL) Western blotting detection reagents (Santa Cruz Biotechnology).

Immunohistochemical staining. Specimens were retrieved from the patients during surgical resection. Archival tumor blocks were fixed with 10% formaldehyde/phosphate-buffered saline (PBS), and embedded in paraffin. The paraffin-embedded tissues, measuring 4 μm in thickness, were placed on glass slides (Matsunami Glass, Osaka, Japan) and deparaf-

Table IV. Comparison of the gene expression levels between human mesenchymal stem cells (hMSCs) and Ewing's sarcoma (EWS) cells.

A.	hMSC		EWS
DKFZP564O0823	–		+
ADAMTS4	–		+
DNER	–		+
NGFR	–		+
LRRN6A	–		+
ECSM2	–		+
LGALS3BP	–		+
PTPRF	–		+
FCGRT	–		+
B.	**hMSC**		**EWS**
LAMP2	+	<	++
RCN1	+	<	+
MMP14	+	<	+
SDC2	+	<	+
DAG1	+	<	+
EPCR	+	<	+
CD97	+	<	+
CD99L2	+	<	+
IGFBP5	+	<	+
CLU	+	<	+
LSAMP	+	<	+
NPTN	+	<	+
EFNA5	+	<	+
PODXL	+	<	+
TMEM123	+	<	+
C.	**hMSC**		**EWS**
PCOLCE	+		+
SEZ6L2	+		+
IGFBP4	+		+
IGFBP3	+		+
LOX	+	>	+
CTGF	+	>	+
SPARC	+	>	+
QSCN6	+	>	+
EDIL3	+		+
MXRA8	+		+
PRRT3	+		+
LRP1	+		+
ISLR	+		+
COL6A1	+	>	+
TIMP1	++	>	+
LAMP1	+		+
SERPINH1	+		+
COL1A1	+		+

++, strongly positive; +, modelately positive; –, negative; >, >2-fold difference in the expression level; <, <2-fold difference in the expression level.

finized in xylene for hematoxylin and eosin (H&E) and immunohistochemical staining. Antigen retrieval was performed with citrate buffer (pH 6.0) at 97˚C for 45 min. After cooling for 60 min and washing in PBS, the rabbit anti-ADAMTS4 antibody (Santa Cruz Biotechnology) diluted 1:50 in antibody diluent buffer (Dako) was reacted. The slides were then washed and incubated with the HRP-conjugated anti-rabbit IgG antibody. The 3-3' diaminobenzidine tetrahydrochloride (DAB) was used for coloration. Hematoxylin was used as the final nuclear counterstaining.

Immunofluorescence staining. The expression of ADAMTS4 protein was analyzed by immunofluorescence. Cells were fixed for 30 min in 4% paraformaldehyde/PBS, and permeabilized for 30 min in 0.1% Triton X/PBS. Fixed cells were rehydrated with Tris-buffered saline, and then incubated with the rabbit polyclonal anti-ADAMTS4 antibody. Immunofluorescence staining was done with the Alexa488-conjugated anti-rabbit IgG antibody. Nucleus was detected with bisbenzimide (Hoechst-33342, Sigma-Aldrich) staining.

ELISA. To evaluate the expression level of secreted ADAMTS4 protein, supernatants of the EWS cell lines and the patient sera were subjected to ELISA. The 96-well plates were coated with the monoclonal anti-human ADAMTS4 antibody at 4˚C overnight. After 3 washes with washing buffer (0.05% Tween-20/PBS), the plates were treated with 10% FBS in PBS for 1 h at room temperature. The recombinant human ADAMTS4 (amino acids 213-685) diluted with 10% FBS in PBS, as standard proteins, and the samples were added to each well, and incubated at room temperature for 2 h. After 5 washes with washing buffer, the Avidin-HRP and the biotinylated anti-human ADAMTS4 detection antibody were added to each well, and incubated for 1 h at room temperature. After 7 washes with washing buffer, 100 μl of tetramethylbenzidine buffer as a substrate was added to each well and incubated for 30 min at room temperature in the dark. Color development was stopped by addition of 100 μl of stop solution (1 N H_3PO_4). Optic density of each sample was measured at 450 nm.

Results

Analysis of isolated cDNA clones. In SST-REX screening, we isolated 322 factor-independent Ba/F3 clones (Table III). Sequencing analyses revealed that integrations derived from 256 clones harbored the signal sequence. Among them, 80 different secreted and type I membrane proteins were identified. We used the database of RefEX, PubMed, ONCOMINE and SMART for the analysis, and 42 proteins that might be related to tumor/cancer onset and progression were selected.

Recent studies have suggested that the origin of EWS is derived from hMSC (40,41). To examine the expression levels of these 42 molecules in EWS in comparison with hMSC, we performed RT-PCR analysis (Table IV). They were classified into 3 groups by mRNA expression profiles; the first group with high expression levels only in EWS (Table IVA), the second group with higher expression levels in EWS than in hMSC (Table IVB), and the third group with similar or lower expression levels in EWS compared with

Table V. Gene expression levels in murine tissues by RT-PCR analysis.

	Brain	Heart	Lung	Liver	Kidney	Spl	Stm	S. int	L. int	Mus	Tes	Thy	BM	OC
DKFZP564O0823	+	+	+	–	+	+	+	+	+	+	+	+	+	+
ADAMTS4	++	+	–	+	–	–	–	–	–	+	–	–	+	+
DNER	++	–	–	–	–	–	–	–	–	–	+	–	–	+
NGFR	+	+	–	+	+	–	–	–	–	–	–	–	–	–
LRRN6A	++	–	–	–	–	+	–	+	+	+	+	+	+	+
ECSM2	+	+	+	+	+	–	+	–	–	+	+	+	+	+
LGALS3BP	+	+	+	+	+	+	+	++	+	+	++	++	+	+
PTPRF	+	+	+	+	+	–	+	+	+	+	+	+	–	–
FCGRT	+	+	+	+	+	+	+	+	+	+	+	+	+	+
LAMP2	+	++	+	+	++	++	+	+	+	+	+	+	+	+
RCN1	+	+	+	+	+	–	+	–	–	–	+	+	+	+
MMP14	+	+	+	+	+	–	+	–	–	+	+	+	+	+
SDC2	+	+	+	+	+	–	+	+	–	+	+	+	+	+
DAG1	+	+	+	+	+	+	+	+	+	+	+	+	+	+
EPCR	+	+	+	+	+	+	+	–	–	+	+	+	+	++
CD97	+	+	+	+	+	+	+	+	+	+	+	+	+	+
CD99L2	+	+	+	+	+	–	–	–	–	+	+	+	+	+
IGFBP5	+	+	+	+	+	+	+	+	+	+	+	+	+	+
CLU	+	+	+	+	+	+	+	+	–	+	+	+	+	+
LSAMP	++	+	–	+	+	–	+	–	–	–	+	+	+	+
NPTN	+	+	+	+	+	–	+	+	+	+	+	+	+	+
EFNA5	+	+	+	+	+	–	+	+	+	–	+	+	–	–
PODXL	+	+	+	+	+	–	–	–	–	+	–	–	+	–
TMEM123	–	+	–	+	+	–	–	–	–	+	–	–	–	–

Spl, spleen; stm, stomach; s. int, small intestine; l. int, large intestine; mus, muscle; tes, testis; thy, thymus; BM, bone marrow; OC, osteoclast; ++, strongly positive; +, modelately positive; –, negative.

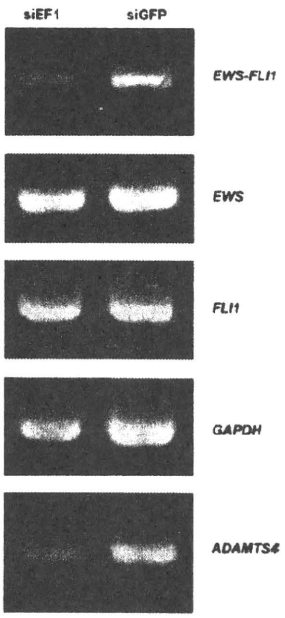

Figure 1. Effects of *EWS-FLI1* suppression on *ADAMTS4* expression. RNA from Ewing's sarcoma cells treated with either siEF1 or siGFP were subjected to RT-PCR experiment. *ADAMTS4* mRNA expression was down-regulated after treatment with *EWS-FLI1*-specific siRNA. *GAPDH* (*glyceraldehyde 3-phosphate dehydrogenase*) was used as an internal control.

hMSC (Table IVC). We picked up 24 molecules from the first and second groups, and examined the expression patterns in murine organs. As shown in Table V, most molecules did not exhibit interesting tissue distribution patterns. However, some of the molecules attracted us by their expression profiles or their novelty as a gene. We focused on 5 molecules: *ADAMTS4*, *DNER* (*δ-notch-like EGF repeat-containing transmembrane*), *NGFR* (*nerve growth factor receptor*), *LRRN6A* (*leucine rich repeat neuronal 6A*) and *ECSM2* (*endothelial cell-specific molecule 2*). We then examined expression levels of these 5 molecules in various solid tumor and hematopoietic cell lines by RT-PCR. As shown in Table VI, expression levels of ADAMTS4 were higher in EWS, glioblastoma and neuroblastoma in comparison with other cell lines. These results suggested that *ADAMTS4* is one of the first candidate molecules as a marker for EWS among the SST clones.

ADAMTS4 expression is upregulated by EWS-FLI1. Previous studies indicated the expression of the fusion gene, EWS-FLI1, was suppressed by using antisense oligonucleotide or siRNA. To decrease the expression level of *EWS-FLI1* in the EWS cell line, we made an siRNA duplex specifically directed against the fusion junction of *EWS-FLI1* transcript. *EWS-FLI1*-specific siRNA (siEF1) was used for SJES-5 cell line. As a control, siGFP was also used. Transfection of siEF1,

Table VI. Gene expression levels of ADAMTS4, DNER, NGFR, LRRN6A and ECSM2 in human cancer cell lines by RT-PCR analysis.

	ADAMTS4	DNER	NGFR	LRRN6A	ECSM2
AsPC-1	–	–	+	–	–
BxPC-3	–	+	–	–	–
Capan-1	–	–	–	–	–
U87MG	+	+	–	–	–
U251	+	++	–	–	–
T98G	–	+	–	–	–
HGC-27	+	–	+	+	–
MKN45	–	+	–	++	–
GCIY	+	+	–	+	–
KATOIII	–	–	–	–	–
MG63	–	+	+	+	+
HOS	+	+	+	+	+
KHOS/NP	–	+	+	+	+
SaOS2	–	+	+	–	–
U2OS	–	+	+	+	–
KPNSI-FA	+	++	+	+	–
LAN-1	+	+	+	+	–
NB69	++	–	+	+	+
H460	+	++	–	+	–
PLC/PRF/5	–	+	+	+	+
HuCCT1	–	++	–	+	+
SW48	–	+	+	–	+
RMS	++	++	+	++	+
SJRH-30	++	+	+	+	+
SJES-2, 3, 5, 6, 7, 8	++	++	+	++	++
MOLM13	–	–	–	–	–
ML1	–	–	–	–	–
U937	–	–	–	–	+
Jurkat	–	–	–	–	+
PEER	–	–	–	–	+
CEM	++	–	–	–	+
HPB-ALL	–	–	–	–	–
NALM24	+	+	–	–	+
NALM16	–	+	+	–	–
IM9	–	–	+	–	+

++, strongly positive; +, moderately positive; –, negative.

but not siGFP, led to significant decrease of the expression level of the *EWS-FLI1* fusion transcript (Fig. 1). In agreement with the specificity of siEF1 against the *EWS-FLI1* fusion gene, the expression level of *EWS* or *FLI1* was not affected. Interestingly, suppression of *EWS-FLI1* expression resulted in decreased expression of *ADAMTS4* transcript. These results suggested that *ADAMTS4* expression was upregulated by EWS-FLI1.

Immunohistochemical analysis on ADAMTS4 protein expression. In order to confirm the expression of ADAMTS4 in EWS at the protein level, we stained 25 tissue samples derived from EWS patients with the anti-ADAMTS4 antibody together with the H&E staining. ADAMTS4 protein was detected in 10 EWS samples, but not in 15 samples where tumors disappeared by chemotherapy (Fig. 2 and data not shown).

Next, to examine the subcellular localization of ADAMTS4, we stained EWS cell lines with the anti-ADAMTS4 antibody. Immunofluorescence microscopy revealed that ADAMTS4 protein was expressed mainly in the cytoplasm of EWS cell lines (Fig. 3C and D) and of the

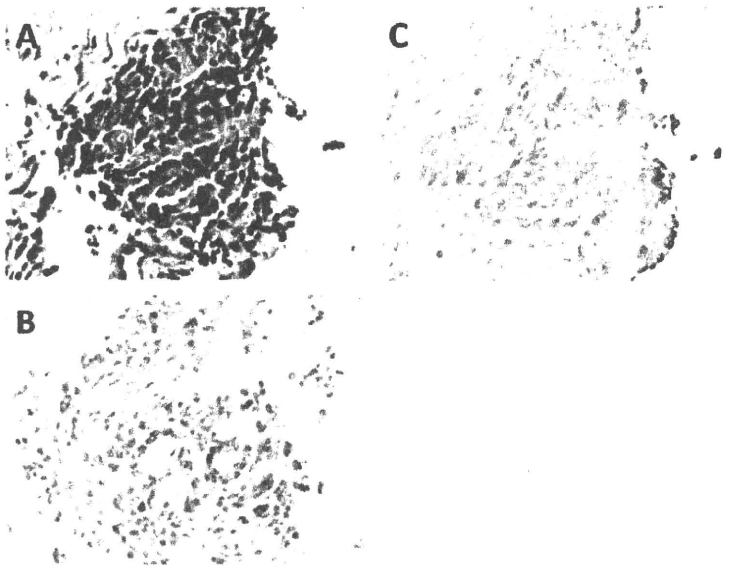

Figure 2. Immunohistochemical analysis of ADAMTS4 protein in the tissue section of the patient with Ewing's sarcoma. (A) Hematoxylin and eosin staining, (B) rabbit IgG, (C) anti-ADAMTS4 antibody.

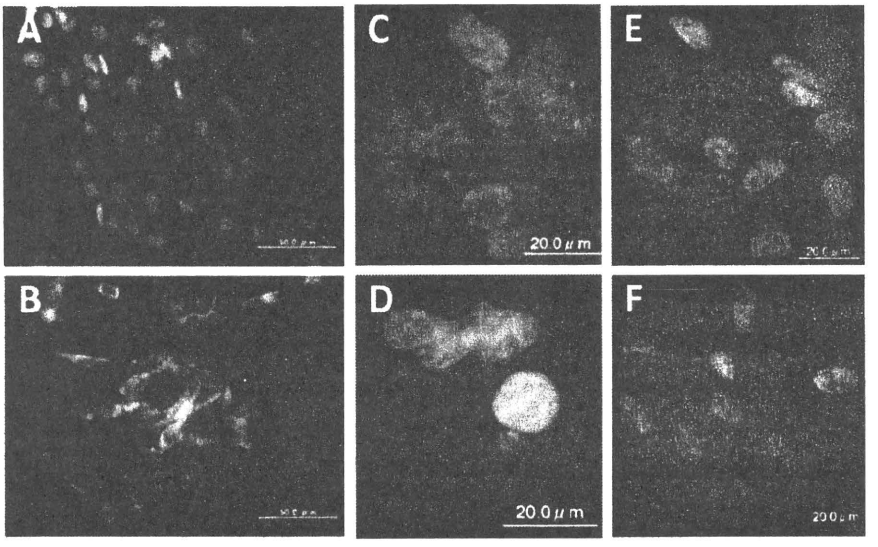

Figure 3. Immunofluorescence staining of ADAMTS4 protein in Ewing's sarcoma cell lines (SJES-2 and SJES-5), osteosarcoma cell lines (MG63 and SaOS2) and NIH3T3 cells expressing ADAMTS4. (A) NIH3T3, (B) ADAMTS4/NIH3T3, (C) SJES-5, (D) SJES-2, (E) MG63, (F) SaOS2.

NIH3T3 cells expressing human ADAMTS4 (Fig. 3B). In contrast, ADAMTS4 was not detected in osteosarcoma cell lines MG63 and SaOS2 (Fig. 3E and F), which did not express *ADAMTS4* at the transcription level (Table VI).

ADAMTS4 is secreted from EWS cells. We next asked whether ADAMTS4 was secreted from EWS cells. First the immunoprecipitates of the cell lysates of EWS cell lines and positive and negative control cells with the anti-ADAMTS4 antibody were electrophoresed, blotted and probed with the same antibody. ADAMTS4 was detcted in EWS cells and the positive control cells as double bands of ~100 kDa (Fig. 4A). We next performed the same experiments using 2 ml each of the supernatants of these cells. Notably, significant levels of expression of ADAMTS4 protein were observed in the supernatants of EWS cells and ADAMTS4/NIH3T3 cells (Fig. 4B). These results suggested that ADAMTS4 was secreted.

Comparative study of ADAMTS4 gene expression in 5 types of sarcomas. We showed that ADAMTS4 transcripts were expressed in EWS, osteosarcoma and rhabdomyosarcoma cell lines (Table VI). However, whether *ADAMTS4* transcripts are expressed in tumor tissue samples remained unknown. Therefore, we tested if *ADAMTS4* was expressed in soft tissue sarcomas and bone tumors including osteosarcoma, EWS, chondrosarcoma, synovial sarcoma and rhabdomyosarcoma (Fig. 5). Benign tumors including lipoma, desmoid

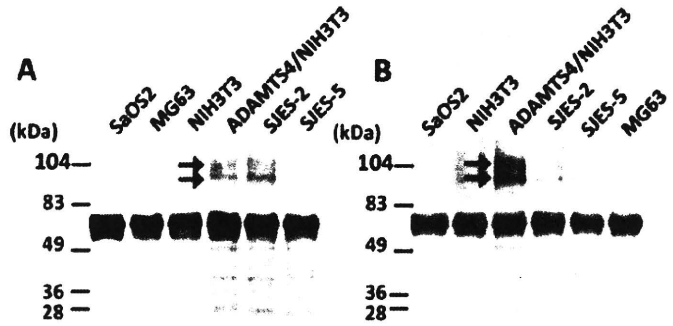

Figure 4. Detection of secreted ADAMTS4 protein. The cell lysates or culture supernatants were immunoprecipitated with the anti-ADAMTS4 antibody, resolved by SDS-PAGE, blotted and probed with the anti-ADAMTS4 antibody. Molecular size markers are shown on the left. Arrows indicate the ADAMTS4 proteins. (A), cell lysates; (B), supernatants.

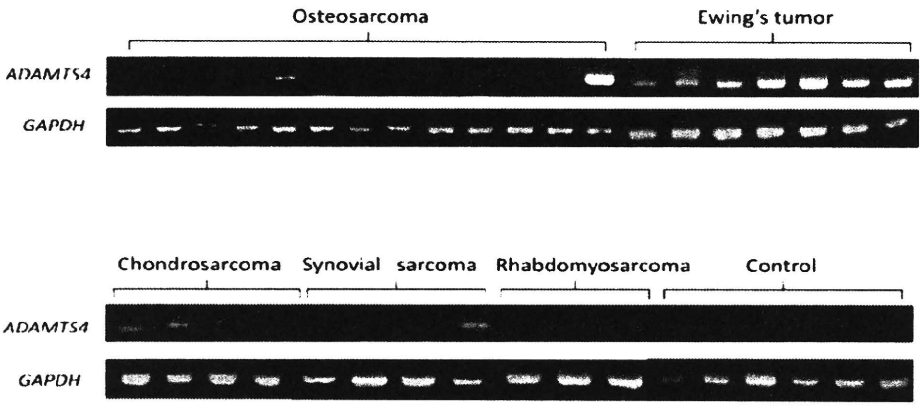

Figure 5. RT-PDR analysis of *ADAMTS4* expression in the patient samples. *GAPDH* expression was used as an internal control.

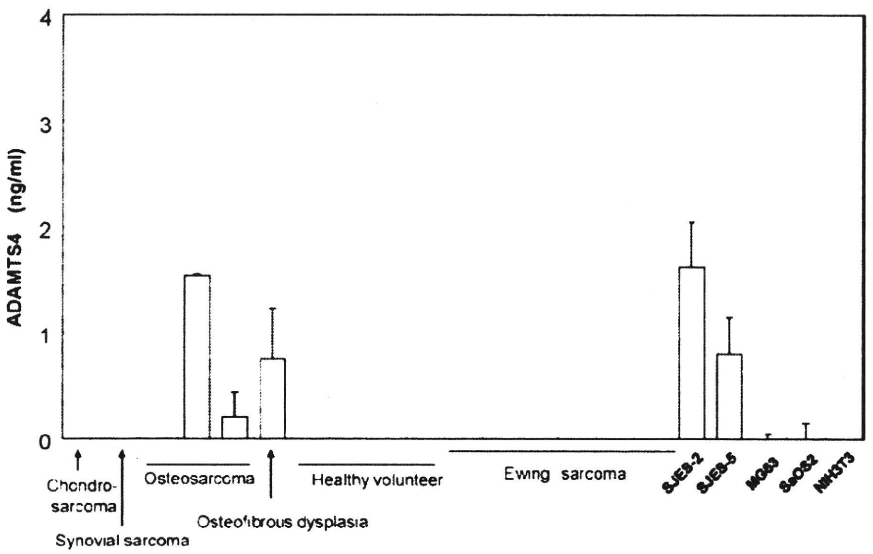

Figure 6. ELISA of ADAMTS4 protein in the patient sera and the supernatants of the cell lines. The error bars represent 1 standard deviation.

and Schwannoma were also examined as controls. In all 7 EWS samples, *ADAMTS4* transcripts were highly expressed. Three out of 4 samples of chondrosarcoma moderately expressed *ADAMTS4*. This result was predictable, since *ADAMTS4* is expressed in normal cartilage cells. Also, 2 out of 13 samples of osteosarcoma and 1 out of 4 samples of synovial sarcoma expressed *ADAMTS4*. *ADAMTS4* transcripts were not detected in the 3 samples of rhabdomyo-

sarcoma, while those were highly expressed in rhabdomyosarcoma cell lines RMS and SJRH-30 (Table VI). Benign tumors examined did not express *ADAMTS4*.

No detection of secreted ADAMTS4 protein in the patient sera. To evaluate the amount of secreted ADAMTS4 protein in the patients, we analyzed ADAMTS4 protein levels in sera by ELISA. In agreement with the results described above, ADAMTS4 was detected in culture supernantants of EWS cell lines SJES-2 and SJES-5 (Fig. 6). The concentration of ADAMTS4 in SJES-2 cells was about twice as high as that in SJES-5 cells. For a positive control, culture supernatant of the NIH3T3/ADAMTS4 cells was also measured (39.9 ng/ml, data not shown). It is noteworthy that ADAMTS4 protein was detected in 2 out of 3 cases of osteosarcoma and in the only case of osteofibrous dysplasia. Consistent with the very high level of *ADAMTS4* transcript shown in the extreme right lane among osteosarcoma samples in Fig. 5, serum from the same patient showed the high level of ADAMTS4 protein in ELISA as shown in Fig. 6 (middle lane among osteosarcoma samples). The other positive samples of osteosarcoma in both figures are not derived from the same patient, because only either serum or RNA was available in these two patients. ADAMTS4 protein was not detected in the 6 EWS patient sera examined. These results indicated that ADAMTS4 is expressed and secreted in EWS cells, but that the ADAMTS4 serum is not suitable as a marker for EWS.

Discussion

EWS is an aggressive neoplasm with a strong propensity to spread into neighboring tissues. Many patients are diagnosed at advanced stages of EWS. Since EWS has worse prognosis than other soft-tissue sarcomas, it is clinically important to distinguish EWS from other sarcomas. The reason for the poor prognosis in EWS patients is suggested to be that the micro-metastases are formed before clinical symptoms arise and tumors are detected (42). Currently, diagnosis of EWS is determined mainly by CD99 expression or by genetic aberrations that are exemplified by *EWS-FLI1* fusion gene. Since both markers show lack of sensitivity, specificity or feasibility, more useful biomarkers such as surface antigens or secreted proteins are required in clinical areas.

In the present study, we searched for membrane and secreted proteins derived from EWS cell lines using the retrovirus-mediated signal sequence trap method SST-REX, and identified ADAMTS4 as a possible EWS marker. We demonstrated that ADAMTS4 was expressed in EWS cell lines and tissue samples derived from EWS patients. Interestingly, expression of *ADAMTS4* was correlated with expression of *EWS-FLI1*, which is a hallmark of EWS. In addition, we demonstrated that ADAMTS4 was secreted from EWS cells, although we could not detect ADAMTS4 in serum samples derived from EWS patients.

It should be noted that two cases of the osteosarcoma patient samples were found to express high levels of *ADAMTS4*. It is tempting to speculate that a subclass of osteosarcoma with different property may exist.

In conclusion, we identified *ADAMTS4* as a possible marker of EWS by using SST-REX. This is the first report to show the correlation between *ADAMTS4* and EWS. Although ADAMTS4 serum could not be used as a biomarker for EWS, our study suggested that RNA transcripts of *ADAMTS4* in the tissue sections are useful markers of EWS. Further studies will be required to determine the usefulness of this molecule in differential diagnosis and/or evaluation of the disease activity in clinical settings.

Acknowledgements

We gratefully thank Ms. S. Shoma (The University of Tokyo) for technical support and Dr Y. Murakami (The University of Tokyo) and Dr Y. Fukuchi (Keio University) for helpful comments on this study. This work was supported by a Grant-in-Aid for Cancer Research from the Ministry of Health, Labour and Welfare of Japan.

References

1. Jaffe R, Santamaria M, Yunis EJ, Tannery NH, Agostini RM, Medina J Jr and Goodman M: The neuroectodermal tumor of bone. Am J Surg Pathol 8: 885-898, 1984.
2. Hashimoto H, Enjoji M, Nakajima T, Kiryu H and Daimaru Y: Malignant neuroepithelioma (peripheral neuroblastoma). A clinicopathologic study of 15 cases. Am J Surg Pathol 7: 309-318, 1983.
3. Khoury JD: Ewing sarcoma family of tumors. Adv Anat Pathol 12: 212-220, 2005.
4. Turc-Carel C, Philip I, Berger MP, Philip T and Lenoir G: Chromosomal translocation (11; 22) in cell lines of Ewing's sarcoma. C R Seances Acad Sci III 296: 1101-1103, 1983.
5. Zucman J, Delattre O, Desmaze C, *et al*: Cloning and characterization of the Ewing's sarcoma and peripheral neuroepithelioma t(11;22) translocation breakpoints. Genes Chromosomes Cancer 5: 271-277, 1992.
6. Sorensen PH, Lessnick SL, Lopez-Terrada D, Liu XF, Triche TJ and Denny CT: A second Ewing's sarcoma translocation, t(21:22), fuses the EWS gene to another ETS-family transcription factor, ERG. Nat Genet 6: 146-151, 1994.
7. Jeon IS, Davis JN, Braun BS, Sublett JE, Roussel MF, Denny CT and Shapiro DN: A variant Ewing's sarcoma translocation (7;22) fuses the EWS gene to the ETS gene ETV1. Oncogene 10: 1229-1234, 1995.
8. Arvand A and Denny CT: Biology of EWS/ETS fusions in Ewing's family tumors. Oncogene 20: 5747-5754, 2001.
9. May WA, Gishizky ML, Lessnick SL, Lunsford LB, Lewis BC, Delattre O, Zucman J, Thomas G and Denny CT: Ewing sarcoma 11;22 translocation produces a chimeric transcription factor that requires the DNA-binding domain encoded by FLI1 for transformation. Proc Natl Acad Sci USA 90: 5752-5756, 1993.
10. Ohno T, Rao VN and Reddy ES: EWS/Fli-1 chimeric protein is a transcriptional activator. Cancer Res 53: 5859-5863, 1993.
11. Jambhekar NA, Bagwan IN, Ghule P, Shet TM, Chinoy RF, Agarwal S, Joshi R and Amare Kadam PS: Comparative analysis of routine histology, immunohistochemistry, reverse transcriptase polymerase chain reaction, and fluorescence in situ hybridization in diagnosis of Ewing family of tumors. Arch Pathol Lab Med 130: 1813-1818, 2006.
12. Llombart-Bosch A and Navarro S: Immunohistochemical detection of EWS and FLI-1 proteinss in Ewing sarcoma and primitive neuroectodermal tumors: comparative analysis with CD99 (MIC-2) expression. Appl Immunohistochem Mol Morphol 9: 255-260, 2006.
13. Bernstein M, Kovar H, Paulussen M, Randall RL, Schuck A, Teot LA and Juergens H: Ewing's sarcoma family of tumors: current management. Oncologist 11: 503-519, 2006.
14. Folpe AL, Hill CE, Parham DM, O'Shea PA and Weiss SW: Immunohistochemical detection of FLI-1 protein expression: a study of 132 round cell tumors with emphasis on CD99-positive mimics of Ewing's sarcoma/primitive neuroectodermal tumor. Am J Surg Pathol 24: 1657-1662, 2000.
15. Bernard G, Zoccola D, Deckert M, Breittmayer JP, Aussel C and Bernard A: The E2 molecule (CD99) specifically triggers homotypic aggregation of $CD4^+$ $CD8^+$ thymocytes. J Immunol 154: 26-32, 1995.

16. Zhang PJ, Barcos M, Stewart CC, Block AW, Sait S and Brooks JJ: Immunoreactivity of MIC2 (CD99) in acute myelogenous leukemia and related diseases. Mod Pathol 13: 452-458, 2000.
17. Tashiro K, Tada H, Heilker R, Shirozu M, Nakano T and Honjo T: Signal sequence trap: a cloning strategy for secreted proteins and type I membrane proteins. Science 261: 600-603, 1993.
18. Shirozu M, Nakano T, Inazawa J, Tashiro K, Tada H, Shinohara T and Honjo T: Structure and chromosomal localization of the human stromal cell-derived factor 1 (SDF1) gene. Genomics 28: 495-500, 1995.
19. Kojima T, Morikawa Y, Copeland NG, Gilbert DJ, Jenkins NA, Senba E and Kitamura T: TROY, a newly identified member of the tumor necrosis factor receptor superfamily, exhibits a homology with Edar and is expressed in embryonic skin and hair follicles. J Biol Chem 275: 20742-20747, 2000.
20. Ohta K, Lupo G, Kuriyama S, Keynes R, Holt CE, Harris WA, Tanaka H and Ohnuma S: Tsukushi functions as an organizer inducer by inhibition of BMP activity in cooperation with chordin. Dev Cell 7: 347-358, 2004.
21. Ikeda Y, Imai Y, Kumagai H, Nosaka T, Morikawa Y, Hisaoka T, Manabe I, Maemura K, Nakaoka T, Imamura T, Miyazono K, Komuro I, Nagai R and Kitamura T: Vasorin, a transforming growth factor beta-binding protein expressed in vascular smooth muscle cells, modulates the arterial response to injury in vivo. Proc Natl Acad Sci USA 101: 10732-10737, 2004.
22. Izawa K, Kitaura J, Yamanishi Y, Matsuoka T, Oki T, Shibata F, Kumagai H, Nakajima H, Maeda-Yamamoto M, Hauchins JP, Tybulewicz VL, Takai T and Kitamura T: Functional analysis of activating receptor LMIR4 as a counterpart of inhibitory receptor LMIR3. J Biol Chem 282: 17997-18008, 2007.
23. Ganju RK, Brubaker SA, Meyer J, Dutt P, Yang Y, Qin S, Newman W and Groopman JE: The alpha-chemokine, stromal cell-derived factor-1alpha, binds to the transmembrane G-protein-coupled CXCR-4 receptor and activates multiple signal transduction pathways. J Biol Chem 273: 23169-23175, 1998.
24. Kitamura T, Onishi M, Kinoshita S, Shibuya A, Miyajima A and Nolan GP: Efficient screening of retroviral cDNA expression libraries. Proc Natl Acad Sci USA 92: 9146-9150, 1995.
25. Kojima T and Kitamura T: A signal sequence trap based on a constitutively active cytokine receptor. Nat Biotechnol 17: 487-490, 1999.
26. Kuno K, Kanada N, Nakashima E, Fujiki F, Ichimura F and Matsushima K: Molecular cloning of a gene encoding a new type of metalloproteinase-disintegrin family protein with thrombospondin motifs as an inflammation associated gene. J Biol Chem 272: 556-562, 1997.
27. Porter S, Clark IM, Kevorkian L and Edwards DR: The ADAMTS metalloproteinases. Biochem J 386: 15-27, 2005.
28. Tortorella MD, Burn TC, Pratta MA, *et al*: Purification and cloning of aggrecanase-1: a member of the ADAMTS family of proteins. Science 284: 1664-1666, 1999.
29. Tortorella MD, Malfait AM, Deccico C and Arner E: The role of ADAM-TS4 (aggrecanase-1) and ADAM-TS5 (aggrecanase-2) in a model of cartilage degradation. Osteoarthritis Cartilage 9: 539-552, 2001.
30. Sandy JD, Neame PJ, Boynton RE and Flannery CR: Catabolism of aggrecan in cartilage explants. Identification of a major cleavage site within the interglobular domain. J Biol Chem 266: 8683-8685, 1991.
31. Sandy JD, Flannery CR, Neame PJ and Lohmander LS: The structure of aggrecan fragments in human synovial fluid. Evidence for the involvement in osteoarthritis of a novel proteinase which cleaves the Glu 373-Ala 374 bond of the interglobular domain. J Clin Invest 89: 1512-1516, 1992.
32. Lohmander LS, Neame PJ and Sandy JD: The structure of aggrecan fragments in human synovial fluid. Evidence that aggrecanase mediates cartilage degradation in inflammatory joint disease, joint injury, and osteoarthritis. Arthritis Rheum 36: 1214-1222, 1993.
33. Kashiwagi M, Tortorella M, Nagase H and Brew K: TIMP-3 is a potent inhibitor of aggrecanase 1 (ADAM-TS4) and aggrecanase 2 (ADAM-TS5). J Biol Chem 276: 12501-12504, 2001.
34. Yamanishi Y, Boyle DL, Clark M, Maki RA, Tortorella MD, Arner EC and Firestein GS: Expression and regulation of aggrecanase in arthritis: the role of TGF-beta. J Immunol 168: 1405-1412, 2002.
35. Matthews RT, Gary SC, Zerillo C, Pratta M, Solomon K, Arner EC and Hockfield S: Brain-enriched hyaluronan binding (BEHAB) brevican cleavage in a glioma cell line is mediated by a disintegrin and metalloproteinase with thrombospondin motifs (ADAMTS) family member. J Biol Chem 275: 22695-22703, 2000.
36. Morita S, Kojima T and Kitamura T: Plat-E: an efficient and stable system for transient packaging of retroviruses. Gene Ther 7: 1063-1066, 2000.
37. Kitamura T, Koshino Y, Shibata F, Oki, T, Nakajima H, Nosaka T and Kumagai H: Retrovirus-mediated gene transfer and expression cloning: powerful tools in functional genomics. Exp Hematol 11: 1007-1014, 2003.
38. Prieur A, Tirode F, Cohen P and Delattre O: EWS FLI-1 silencing and gene profiling of Ewing cells reveal downstream oncogenic pathways and a crucial role for repression of insulin-like growth factor binding protein 3. Mol Cell Biol 24: 7275-7283, 2004.
39. Nosaka T, Kawashima T, Misawa K, Ikuta K, Mui AL and Kitamura T: STAT5 as a molecular regulator of proliferation, differentiation and apoptosis in hematopoietic cells. EMBO J 18: 4754-4765, 1999.
40. Tirode F, Laud-Duval K, Prieur A, Delorme B, Charbord P and Delattre O: Mesenchymal stem cell features of Ewing tumors. Cancer Cell 11: 421-429, 2007.
41. Riggi N, Cironi L, Provero P, Suva ML, Kaloulis K, Garcia-Echeverria C, Hoffmann F, Trumpp A and Stamenkovic I: Development of Ewing's sarcoma from primary bone marrow-derived mesenchymal progenitor cells. Cancer Res 65: 11459-11468, 2005.
42. Schleiermacher G, Peter M, Oberlin O, Philip T, Rubie H, Mechinaud F, Sommelet-Olive D, Landman-Parker J, Bours D, Michon J and Delattre O: Increased risk of systemic relapses associated with bone marrow micrometastasis and circulating tumor cells in localized Ewing tumor. J Clin Oncol 21: 85-91, 2003.

Molecular Genetics and Metabolism 100 (2010) 339–344

Contents lists available at ScienceDirect

Molecular Genetics and Metabolism

journal homepage: www.elsevier.com/locate/ymgme

A novel mutation (c.951C>T) in an exonic splicing enhancer results in exon 10 skipping in the human mitochondrial acetoacetyl-CoA thiolase gene

Toshiyuki Fukao [a,b,*], Reiko Horikawa [c], Yasuhiro Naiki [c], Toju Tanaka [d], Masaki Takayanagi [e], Seiji Yamaguchi [f], Naomi Kondo [a]

[a] Department of Pediatrics, Graduate School of Medicine, Gifu University, Gifu 501-1194, Japan
[b] Medical Information Sciences Division, United Graduate School of Drug Discovery and Medical Information Sciences, Gifu University, Gifu 501-1196, Japan
[c] Division of Endocrinology and Metabolism, National Center for Child Health and Development, Tokyo 157-8535, Japan
[d] Division of Clinical Genetics and Molecular Medicine, National Center for Child Health and Development, Tokyo 157-8535, Japan
[e] Chiba Children's Hospital, Chiba 266-0007, Japan
[f] Department of Pediatrics, Faculty of Medicine, Shimane University, Izumo, Shimane 693-8501, Japan

ARTICLE INFO

Article history:
Received 9 February 2010
Received in revised form 16 March 2010
Accepted 16 March 2010
Available online 19 March 2010

Keywords:
Aberrant splicing
Exonic mutation
Splice site selection
Mitochondrial acetoacetyl-CoA thiolase
Inborn error of metabolism
SF2/ASF

ABSTRACT

Mitochondrial acetoacetyl-CoA thiolase (T2) deficiency is an inherited disorder affecting isoleucine catabolism and ketone body metabolism. A Japanese female developed a severe ketoacidotic attack at the age of 7 months. Urinary organic acid analysis showed elevated excretion of 2-methyl-3-hydroxybutyrate but not tiglylglycine. She was diagnosed as having T2 deficiency by enzyme assay using fibroblasts. Mutation analysis revealed a compound heterozygote of c.556G>T(D186Y) and c.951C>T(D317D). Since c.951C>T does not cause amino acid change, we performed cDNA analysis and found that exon 10 skipping had occurred in the c.951C>T allele. A computer search using an ESE finder showed that an exonic splicing enhancer sequence, SF2/ASF, was located in CTGA^{951}CGC. We hypothesized that the exonic splicing enhancer is necessary for accurate splicing since the first nucleotide of exon 10 is C, which weakens the splice acceptor site of intron 9. We made a mini gene construct including exon 9-truncated intron 9-exon 10-truncated intron 10-exon 11 for a splicing experiment. We also made three mutant constructs which alter the SF2/ASF site (947C>T, 951C>T, 952G>A). An min-gene splicing experiment clearly showed that exon 10 skipping was induced in all three mutant constructs. Moreover, additional substitution of G for C at the first nucleotide of exon 10 resulted in normal splicing in these three mutants. These results confirmed that c.951C>T diminished the effect of the exonic splicing enhancer and caused exon 10 skipping.

Introduction

Mitochondrial acetoacetyl-CoA thiolase (T2[1]) (EC 2.3.1.9, gene symbol *ACAT1*) deficiency (OMIM 203750, 607809) is an autosomal recessive disorder, commonly known as β-ketothiolase deficiency. Since 1971 [1], more than 70 patients with it have been identified (including personal communications) [2]. This disorder affects the catabolism of isoleucine and the metabolism of ketone bodies, and is clinically characterized by intermittent ketoacidotic episodes with no clinical symptoms between episodes. T2-deficient patients usually have urinary excretion of 2-methyl-3-hydroxybutyrate, 2-methylacetoacetate and tiglylglycine, derived from intermediates in isoleucine catabolism. The severity of the clinical features varies from patient to patient but follow-up studies reveal that, in general, T2 deficiency has a favorable outcome [3].

The T2 gene (gene symbol: ACAT1) spans approximately 27 kb, contains 12 exons [4], and is located at 11q22.3–q23.1 [5]. Human T2 cDNA is about 1.5 kb long and encodes a precursor protein of 427 amino acids, including a 33-amino-acid leader polypeptide [6]. We have identified more than 70 gene mutations [7–25], 15% of which cause aberrant splicing. Most were located at the highly conserved ag at the splice acceptor site and gt at the splice donor site. We also identified some exonic mutations which cause aberrant splicing by activating cryptic splice sites within their exons [15,24].

We herein report a novel exonic mutation—c.951C>T (the 11th nucleotide in exon 10). It was first regarded to be a silent mutation, D317D, but was associated with exon 10 skipping in cDNA analysis. The c.951C nucleotide is located in a possible exonic splicing enhancer (ESE) sequence, SF2/ASF, and C>T substitution results in a deviation from its consensus sequence. We showed by a

* Corresponding author at: Department of Pediatrics, Graduate School of Medicine, Gifu University, 1-1 Yanagido, Gifu 501-1194, Japan. Fax: +81 58 230 6387.
E-mail address: toshi-gif@umin.net (T. Fukao).

[1] *Abbreviation used:* T2, mitochondrial acetoacetyl-CoA thiolase.

1096-7192/$ - see front matter © 2010 Elsevier Inc. All rights reserved.
doi:10.1016/j.ymgme.2010.03.012

minigene splicing experiment that the substitutions in this ESE caused exon 10 skipping.

Materials and methods

Case report

The patient (GK64), a female, was born to non-consanguineous Japanese parents. She was well until 7 months of age when she presented with a one-week history of coughing and appetite loss. She developed convulsions and was admitted to a hospital. Laboratory findings showed blood pH 6.769, bicarbonate 2.8 mmol/L, base excess −28.2 mmol/L, ammonia 213 μmol/L, and blood glucose 0.45 mmol/L. She was referred to the National Center for Child Health and Development on a mechanical ventilation support. Urinary organic acid analysis at the time of crisis showed huge amounts of acetoacetate and 3-hydroxybutyrate with dicarboxylic acids; 2-methyl-3-hydroxybutyrate and tiglylglycine were not evident at that time. She was successfully treated by intravenous glucose infusion. Later, she had an upper respiratory infection and her urinary ketone was 2+ at the age of 8 months. At that time, urinary organic acid analysis showed the presence of 2-methyl-3-hydroxybutyrate. However, tiglylglycine, another characteristic urinary organic acid in T2 deficiency, was not detected. Skin biopsy and a fibroblast culture were performed and finally she was diagnosed as having T2 deficiency by enzyme assay.

Cell culture, enzyme assay and immunoblot analysis

The fibroblasts were cultured in Eagle's minimum essential medium containing 10% fetal calf serum. Acetoacetyl-CoA thiolase activity was assayed, as described in [26]. Immunoblot analysis was done, as described in [27].

Mutation detection

Genomic DNA was purified from the fibroblasts with Sepa Gene kits (Sanko Junyaku, Tokyo, Japan). Mutation screening was performed at the genomic level by PCR and direct sequencing using a primer set for 12 fragments including an exon and its intron boundaries [13]. RNA was prepared from the fibroblasts using an ISOGEN kit (Nippon Gene, Tokyo, Japan). RT-PCR and sequencing after subcloning into a pGEM-T Easy vector (Promega, Madison, USA) were performed as described previously [7], except for the following point. A full-coding sequence of human T2 cDNA was amplified as a single fragment using a sense primer (5′-$^{-40}$AGTCTACGCCTGTGGAGCCGA^{-20}-3′) and an antisense primer (5′-^{1326}TTCTGGTCACATAGGGTT^{1309}-3′).

Transient expression analyses

Transient expression analysis of T2 cDNAs was done using a pCAGGS eukaryote expression vector [28], as described in [19]. After transfection, the cells were further cultured at 37 °C for 72 h, and then they were harvested and kept at −80 °C until use. The cells were freeze-thawed and sonicated in 50 mM sodium phosphate (pH 8.0), 0.1% Triton X-100. After centrifugation at 10,000*g* for 10 min, the supernatant was used in an enzyme assay for acetoacetyl-CoA thiolase activity and for immunoblot analysis.

Splicing experiment

A fragment (about 4 kb long) from the middle part of exon 9 to the middle part of exon 11 was amplified by Phusion DNA polymerase (New England BioLabs, Ipswich, USA) using control genomic DNA. The primers used in this amplification included the EcoR I linker sequence, as follows:

Ex 9 (EcoR I) primer (exon 9, sense) 5′-cagctgcgaatt^{842}CCAGTAC ACTGAATGATGGAGCAGCT^{873}-3′.

Ex 11 (EcoR I) primer (exon 11, antisense) 5′-cctccattggaatt^{1122}C ACTTTTTGGGGATCAATCT^{1103}-3′.

The amplified fragment, after digestion with EcoR I, was subcloned into an EcoR I site of the pCAGGS expression vector from which the Hind III and Pst I sites were deleted. The subcloned PCR fragment did not contain PCR errors, at least in the sequence of exon 9, the 3′ and 5′ splice sites of intron 9, exon 10, the 3′ and 5′ splice sites of intron 10, and exon 11. We deleted about a 0.5-kb Hind III-Pst I inner fragment in intron 9 and a 1.1-kb Hind III-Pst I inner fragment in intron 10 to reduce the minigene construct length. In order to make an mutant construct, in vitro mutagenesis was done on the wild-type fragment in the pUC118 vector, and then the mutant fragment was subcloned into the pCAGGS expression vector as a cassette of an about 870-bp Pst I-Hind III fragment including exon 10. We made three mutant constructs which altered the SF2/ASF site (c.947C>T, c.951C>T, and c.952G>A). Moreover, we also made three further mutant constructs with additional substitution of c.941G for C at the first nucleotide of exon 10.

Two μg of these expression vectors were transfected into 5×10^5 cells of SV40-transformed fibroblasts using Lipofectamine 2000. At 48 h after transfection, RNA was extracted from the cells. The first-strand cDNA was transcribed with a rabbit β-globin-specific antisense primer (β-glo2) (5′-^{461}AGCCACCACCTTCTGATA-3′) and then amplified with the Ex10 (EcoRI) primer on T2 exon 10, and another rabbit-specific antisense primer (β-glo3) (5′-^{443}GGCAGCCTGCACCTGAGGAGT-3′) to amplify the chimera cDNA of human T2 and rabbit β-globin.

Allele-specific RT-PCR

We performed allele-specific RT-PCR using mismatched primers:

c.556G allele (D186)-specific sense primer, 5′-^{530}TTTGATTGTA AAA GACGGGCTATCTG^{556}-3′.

c.556T allele (Y186)-specific sense primer, 5′-^{530}TTTGATTGTA AAA GACGGGCTATCTT^{556}-3′

The bold G or T represents the D186Y mutation site of c.556G>A. The underlined T indicates a mismatch introduced to the 4th nucleotide to assist allele-specific-RT-PCR.

Antisense primer 5′-^{1065}GGCTTCTTTACTTCCCACATTGCA^{1041}-3′.

cDNA with exon 10 gave a 535-bp fragment and cDNA with exon 10 skipping gave a 470-bp fragment.

Results and discussion

Enzyme assay and immunoblot analysis

Potassium-ion-activated acetoacetyl-CoA thiolase activity was absent in GK64's fibroblasts ($-K^+$ 3.8, $+K^+$ 3.9 nmol/min/mg of protein; Control fibroblasts $-K^+$ 4.7, $+K^+$ 7.8 nmol/min/mg of protein), confirming the diagnosis of T2 deficiency. Succinyl-CoA:3-ketoacid CoA transferase activity was 6.3 nmol/min/mg of protein (control fibroblasts 5.6 nmol/min/mg of protein). In immunoblot analysis, GK64's fibroblasts had a reduced but significant amount of T2 protein (Fig. 1). We then performed immunoblot analysis using twofold serially diluted samples of two controls and GK64's fibroblasts from 30 to 3.75 μg. The relative amount of T2 protein in GK64 fibroblasts were estimated to be 25% of controls (data not shown).

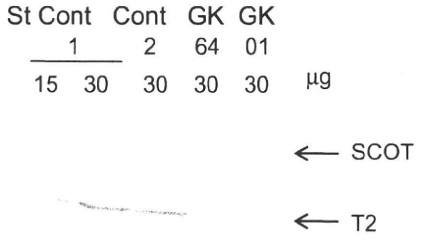

Fig. 1. Immunoblot analysis. The amount of fibroblast protein extract applied was indicated in each lane. The first antibody was a mixture of an anti-T2 antibody and an anti-SCOT antibody. The positions of the bands for T2 and SCOT are indicated by arrows. Cont 1 and Cont 2 were healthy controls and GK01 was a disease control being cross reactive material-negative.

Mutation screening at the genomic level and cDNA level

Routine genomic PCR and sequencing of exons 1–12 identified two nucleotide substitutions, c.556G>T(D186Y) in exon 6 and c.951C>T(D317D) in exon 10. Both c.556G>T and c.951C>T were novel nucleotide substitutions in the T2 gene. No further mutations were identified by genomic mutation screening. Since the latter substitution does not alter amino acid, we performed RT-PCR analysis. A full-coding region was amplified using a pair of primers on a 5′-noncoding region and a 3′-non-coding region, allowing one to show the segregation of these two substitutions. After subcloning, 8 clones had c.556G>T(D186Y) but not c.951C>T(D317D). Two clones had exon 10 skipping without c.556G>T(D186Y). The exon 10 skipping causes a frame shift and premature termination at c.1011TAA. We re-sequenced the genomic region around exon 10 (IVS8 − 88–IVS9 + 44) again, but only c.951C>T(D317D) was detected. We regarded c.951C>T(D317D), the 11th nucleotide of exon 10, as the cause of exon 10 skipping which was detected in GK64's cDNA. Since the splice acceptor site of intron 9 might be weak because of the first nucleotide of exon 10 being C, we hypothesized that ESE sequences would be necessary for accurate exon recognition of exon 10 and that c.951C>T might disrupt the ESE and result in exon 10 skipping.

Transient expression analysis of D186Y mutant cDNA

Transfection of wild-type T2 cDNA gave a high acetoacetyl-CoA thiolase activity in the presence of potassium ion. Transfection of D186Y mutant cDNA gave no significant thiolase activity compared with mock cDNA transfection (Fig. 2A) Immunoblot analysis showed that mutant D186Y protein was detected with 1/3-fold amount of wild-type protein (Fig. 2B). These results indicate that the D186Y mutant protein is a stable protein but retains no residual activity. Even when incubation was done at a lower temperature (30 °C) after transfection, no residual T2 activity was detected (data not shown). This result confirmed that the D186Y mutation is a causative mutation in one allele, and is consistent with the fact that GK64's fibroblasts had T2 protein with about a 1/4-fold amount of controls'.

Searches for ESE sequence

We searched the possible ESE sequences which can be affected by c.951C>T, using ESE finder 3.0 (http://rulai.cshl.edu/cgi-bin/tools/ESE3/esefinder.cgi?process=home) [30–31] and found that this mutated site, c.951C>T, was located in a possible SF2/ASF site, c.947CTGA951CGC (7th–13th nucleotides in exon 10). The substitution made a deviation from the consensus sequence of SF2/ASF, as shown in Fig. 3A.

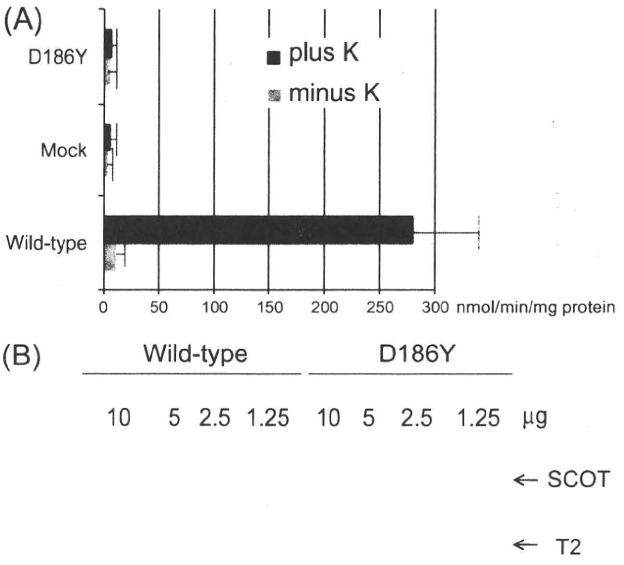

Fig. 2. Transient expression analysis of D186Y mutant cDNA. (A) Potassium-ion-activated acetoacetyl-CoA thiolase assay. Acetoacetyl-CoA thiolase activity in the supernatant of the cell extract was measured. The mean values of acetoacetyl-CoA thiolase activity in the absence and presence of the potassium ion are shown together with the standard deviation of three independent experiments. (B) Immunoblot analysis. The protein amounts applied are shown above the lanes. The first antibody was a mixture of an anti-T2 antibody and an anti-SCOT antibody.

Minigene splicing constructs

We previously successfully performed minigene splicing experiments using a pCAGGS expression vector [8,24,29]. Since our minigene construct produces human T2-rabbit β-globin fusion mRNA, we could amplify this specific mRNA by RT-PCR using a combination of a human T2 sense primer and a rabbit β-globin antisense primer. We made a minigene construct including exon 9-truncated intron 9-exon 10-truncated intron 10-exon 11 for a splicing experiment, as shown in Fig. 3B. We made the c.951C>T mutant constructs and two additional mutant constructs (c.947C>T or c.952G>A) which also altered the SF2/ASF site, as shown in Fig. 3A. We hypothesized that the ESE is necessary for accurate splicing since the first nucleotide of exon 10 is C, which weakens the splice acceptor site of intron 9. Hence, we made three constructs with an additional substitution of 941G for C at the first nucleotide of exon 10 to strengthen the splice acceptor site of intron 9.

Splicing experiment

We performed a minigene splicing experiment. As shown in Fig. 3C, exon 10 skipping was induced in all three mutant constructs. Normally spliced transcripts with the inclusion of exon 10 were also produced in these mutant transcripts. The ratio of signal intensity of transcripts with exon 10 skipping to that of normally spliced transcripts in three independent experiments was highest in c.951C>T, followed by c.952G>A among these three mutants.

Moreover, additional substitution of G for C at the first nucleotide of exon 10 resulted in normal splicing in these three mutants. Hence, the ESE (SF2/ASF) was only necessary in the case of C at the first nucleotide of exon 10 in the experiment. This clearly showed that c.941C, the first nucleotide of exon 10, makes the recognition

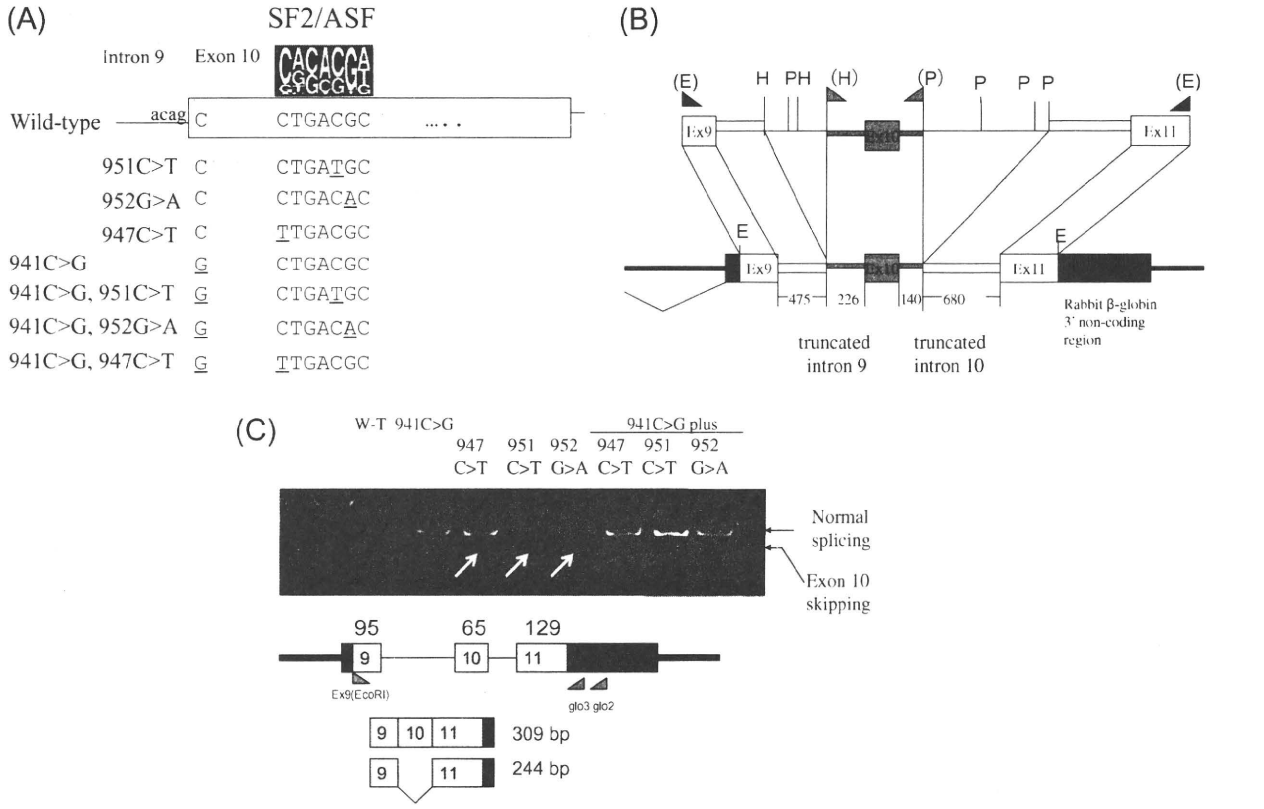

Fig. 3. Minigene splicing experiment. (A) Minigene splicing constructs. Sequence differences among 8 minigene splicing constructs. Mutations introduced are underlined. (B) Schematic presentation of minigene splicing construct. The minigene construct has a T2 gene fragment from c.842 of exon 9 and intron 9 (from +1 to a Hind III site, 475-bp open box) and intron 10 (from a Pst I site to −1, 680-bp open box) and exon 11 (to c. 1122). In the cases of mutant constructs, the region around exon 10, highlighted in gray, was replaced as a cassette. Thick lines and black boxes indicate pCAGGS vector sequences. (C) Detection of chimeric cDNAs derived from transfected minigenes. First-strand cDNA was reverse-transcribed using the glo2 primer. cDNA amplification was done using Ex9(EcoRI) and glo3 primers. Normal splicing and aberrant splicing produced 309-bp and 244-bp PCR fragments, respectively. The PCR fragments were electrophoresed on 5% polyacrylamide gel. Fragments with exon 10 skipping are shown by arrows.

of exon 10 or the splice acceptor site of intron 9 and requires an ESE for the accurate splicing of exon 10. These results confirmed that c.951C>T diminished the effect of the ESE and caused exon 10 skipping.

Effects of c.951C>T mutation on splicing

In the minigene splicing, normally spliced transcripts were detected in the construct with c.951C>T. This may mean that not only exon-10-skipped transcripts but also normally splicied transcripts can be produced in the c.951C>T mutant allele. However, when we analyzed 10 clones of full-length cDNA, 8 clones were from the allele with c.556G>T(D186Y). Two clones had exon 10 skipping but no cDNA clones with c.951C>T were found. In direct sequencing of full-length cDNA fragments, we found a possible faint signal for c.951T in the major signal for c.951C (Fig. 4B). Hence, the presence of normally spliced transcripts from c.951C>T was further confirmed by allele-specific RT-PCR. As shown in Fig. 4A, both c.556T(Y186) allele- and c.556G(D186) allele-specific RT-PCR gave a fragment with the expected size in the case of GK64, and only the latter gave a fragment in the case of a control. In direct sequencing of GK64's fragment of the c.556G(D186) allele, c.951 was T (normally spliced transcripts in the c.951C>T mutant allele) (Fig. 4B). An additional faint fragment with exon 10 skipping was also seen in GK64's c.556G(D186) allele-specific PCR. Exon 10 skipping causes frame shift and should result in nonsense-mediated mRNA decay; hence, the amount of cDNA with exon 10 skipping in the D186 allele was smaller than that of normally spliced cDNA. Based

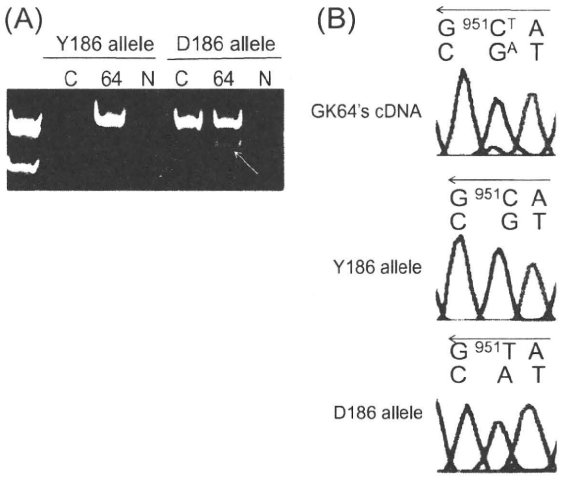

Fig. 4. Allele-specific cDNA amplification. (A) Allele-specific PCR fragments were electrophoresed on 5% polyacrylamide gel. C, control cDNA; 64, GK64's cDNA, N, negative control. An arrow indicates cDNA with exon 10 skipping. (B) Direct sequencing of the antisense strand at the c.951c>T (D186Y) site. Y186 allele, Y186 allele-specific PCR fragment; D186 allele, D186 allele-specific PCR fragment.

on cDNA analysis, a small amount of normally spliced mRNA with c.951C>T(D317D) was also produced and hence GK64 retained some residual T2 activity from this mutant allele. This finding is in accord with GK64's urinary organic acid profiles. We previously

showed that urinary organic acid analysis shows no elevated tiglylglycine and relatively small amount of 2-methyl-3-hydroxybutyrate even during ketoacidotic crisis and subtle elevation of 2-methyl-3-hydroxybutyrate under stable conditions in patients with mutations which retain some residual T2 activity [3,18,19].

The importance of the exonic splicing enhancer

The accurate removal of introns from pre-mRNA is essential for correct gene expression. However, the information contained in splice sites, including the splice donor site, branch site and splice acceptor site, is insufficient for a precise definition of exons [32–35]. Recently, it was established that exon sequence has elements which contribute to exonic recognition. Additional regulatory elements exist in the form of ESEs [32,33]. Exonic variants may inactivate an ESE, resulting in insufficient exon inclusion.

ESEs are known to play a particularly important role in exons with weak splice sites. Although the splice acceptor site of intron 10 has a relatively high Shapiro and Senapathy score [35] of 90.5, the site deviates from the consensus sequence at position +1, by the replacement of the G nucleotide with C. In computer analysis using ESE finder, the mutation c.951C>T was located on an ESE, the SF2/ASF site. SF2/ASF is a prototypical serine- and arginine-rich protein (SR family) with important roles in splicing and other aspects of mRNA metabolism. One classical function of SR proteins bound to exonic sequences is to stimulate recognition of the flanking splice sites [36]. Using the minigene approach, we have demonstrated that not only the c.951C>T substitution but also c.947C>T and c.952G>A, all of which affected the SF2/ASF site, resulted in insufficient exon 10 inclusion. This phenomenon was completely corrected by a substitution of G for C at the first nucleotide of exon 10. We therefore suggest that the weak splice acceptor site of intron 10 is normally compensated for by an ESE (SF2/ASF).

There are several precedent reports on ESE mutations in other genes [37–39]. For example, two synonymous mutations in exon 5 identified in pyruvate dehydrogenase-deficient patients (the c.483C>T and c.498C>T variants) disrupt a putative ESE, the SRp55 binding site [37]. These synonymous mutations result in the incomplete inclusion of PDHA1 exon 5 in the minigene splicing experiment and this effect is corrected following the restoration of a perfect consensus sequence for the 5′ splice site by site-directed mutagenesis. The mutation in the SRp55 binding site is affected in the case of the weak 5′ splice site selection in this case and the mutation in SF2/ASF site was affected in the case of the weak 3′ splice site selection in our case. c.1918C>G (pR640G) in exon 14 in the APC gene, which was found in a familial adenomatous polyposis (FAP) patient, was revealed to be sufficient to cause exon 14 skipping [38]. Minigene splicing experiments showed a mechanism involving disruption of an ASF/SF2 element. Systemic analysis of 24 mutations in PAH exon 9 showed that three of them affected ESE motifs and resulted in exon 9 skipping [39]. These facts indicate that we should consider that any mutations in an exon may affect splicing of the exon.

Importance of cDNA analysis

If mutation analysis were done only at the genomic level, this c.951C>T(D317D) mutation would be regarded as a silent mutation. However, the main character of this mutation was an ESE mutation which causes exon 10 skipping. Any nucleotide substitutions have the possibility to affect splicing efficiency. This indicates the importance of cDNA analysis to understand the character of mutations properly.

Acknowledgments

We thank N. Sakaguchi and K. Murase for technical assistance.

This study was supported in part by a Grant-in-Aid for Scientific Research from the Ministry of Education, Science, Sports and Culture of Japan and by Health and Labor Science Research Grants for Research on Intractable Diseases and For Research on Children and Families from The Ministry of Health, Labor and Welfare of Japan.

References

[1] R.S. Daum, P. Lamm, O.A. Mamer, C.R. Scriver, A "new" disorder of isoleucine catabolism, Lancet 2 (1971) 1289–1290.
[2] G.A. Mitchell, T. Fukao, Chapter 102, Inborn errors of ketone body metabolism, in: C.R. Scriver, A.L. Beaudet, W.S. Sly, D. Valle (Eds.), Metabolic and Molecular Bases of Inherited Disease, eighth ed., McGraw-Hill, Inc., New York, 2001, pp. 2327–2356.
[3] T. Fukao, C.R. Scriver, N. Kondo, T2 Collaborative Working Group, The clinical phenotype and outcome of mitochondrial acetoacetyl-CoA thiolase deficiency (b-ketothiolase deficiency) in 26 enzymatically proved and mutation defined patients, Mol. Genet. Metab. 72 (2001) 109–114.
[4] M. Kano, T. Fukao, S. Yamaguchi, T. Orii, T. Osumi, T. Hashimoto, Structure and expression of the human mitochondrial acetoacetyl-CoA thiolase-encoding gene, Gene 109 (1991) 285–290.
[5] M. Masuno, M. Kano, T. Fukao, S. Yamaguchi, T. Osumi, T. Hashimoto, E. Takahashi, T. Hori, T. Orii, Chromosome mapping of the human mitochondrial acetoacetyl-coenzyme A thiolase gene to 11q22.3–q23.1 by fluorescence in situ hybridization, Cytogenet. Cell Genet. 60 (1992) 121–122.
[6] T. Fukao, S. Yamaguchi, M. Kano, T. Orii, Y. Fujiki, T. Osumi, T. Hashimoto, Molecular cloning and sequence of the complementary DNA encoding human mitochondrial acetoacetyl-coenzyme A thiolase and study of the variant enzymes in cultured fibroblasts from patients with 3-ketothiolase deficiency, J. Clin. Invest. 86 (1990) 2086–2092.
[7] T. Fukao, S. Yamaguchi, T. Orii, R.B.H. Schutgens, T. Osumi, T. Hashimoto, Identification of three mutant alleles of the gene for mitochondrial acetoacetyl-CoA thiolase: a complete analysis of two generations of a family with 3-ketothiolase deficiency, J. Clin. Invest. 89 (1992) 474–479.
[8] T. Fukao, S. Yamaguchi, A. Wakazono, T. Orii, G. Hoganson, T. Hashimoto, Identification of a novel exonic mutation at −13 from 5′ splice site causing exon skipping in a girl with mitochondrial acetoacetyl-coenzyme A thiolase deficiency, J. Clin. Invest. 93 (1994) 1035–1041.
[9] T. Fukao, S. Yamaguchi, T. Orii, T. Hashimoto, Molecular basis of beta-ketothiolase deficiency: mutations and polymorphisms in the human mitochondrial acetoacetyl-coenzyme A thiolase gene, Hum. Mutat. 5 (1995) 113–120.
[10] T. Fukao, X.Q. Song, S. Yamaguchi, T. Orii, R.J.A. Wanders, B.T. Poll-The, T. Hashimoto, Mitochondrial acetoacetyl-coenzyme A thiolase gene: a novel 68-bp deletion involving 3′ splice site of intron 7, causing exon 8 skipping in a Caucasian patient with beta-ketothiolase deficiency, Hum. Mutat. 5 (1995) 94–96.
[11] A. Wakazono, T. Fukao, S. Yamaguchi, Y. Hori, T. Orii, M. Lambert, G.A. Mitchell, G.W. Lee, T. Hashimoto, Molecular and biochemical, and clinical characterization of mitochondrial acetoacetyl-coenzyme A thiolase deficiency in two further patients, Hum. Mutat. 5 (1995) 34–42.
[12] T. Fukao, X.Q. Song, S. Yamaguchi, N. Kondo, T. Orii, J.M. Matthieu, C. Bachmann, T. Orii, Identification of three novel frameshift mutations (83delAT, 754indCT, and 435+1G to A) of mitochondrial acetoacetyl-coenzyme A thiolase gene in two Swiss patients with CRM-negative beta-ketothiolase deficiency, Hum. Mutat. 9 (1997) 277–279.
[13] T. Fukao, H. Nakamura, X.Q. Song, K. Nakamura, K.E. Orii, Y. Kohno, M. Kano, S. Yamaguchi, T. Hashimoto, T. Orii, N. Kondo, Characterization of N93S, I312T, and A333P missense mutations in two Japanese families with mitochondrial acetoacetyl-CoA thiolase deficiency, Hum. Mutat. 2 (1998) 245–254.
[14] A.C. Sewell, J. Herwig, I. Wiegratz, W. Lehnert, H. Niederhoff, X.Q. Song, N. Kondo, T. Fukao, Mitochondrial acetoacetyl-CoA thiolase (beta-keto-thiolase) deficiency and pregnancy, J. Inherit. Metab. Dis. 21 (1998) 441–442.
[15] K. Nakamura, T. Fukao, C. Perez-Cerda, C. Luque, X.Q. Song, Y. Naiki, Y. Kohno, M. Ugarte, N. Kondo, A novel single-base substitution (380C>T) that activates a 5-base downstream cryptic splice-acceptor site within exon 5 in almost all transcripts in the human mitochondrial acetoacetyl-CoA thiolase gene, Mol. Genet. Metab. 72 (2001) 115–121.
[16] T. Fukao, H. Nakamura, K. Nakamura, C. Perez-Cerda, A. Baldellou, C.R. Barrionuevo, F.G. Castello, Y. Kohno, M. Ugarte, N. Kondo, Characterization of 6 mutations in 5 Spanish patients with mitochondrial acetoacetyl-CoA thiolase deficiency: effects of amino acid substitutions on tertiary structure, Mol. Genet. Metab. 75 (2002) 235–243.
[17] T. Fukao, N. Matsuo, G.X. Zhang, R. Urasawa, T. Kubo, Y. Kohno, N. Kondo, Single base substitutions at the initiator codon in the mitochondrial acetoacetyl-CoA thiolase (ACAT1/T2) gene result in production of varying amounts of wild-type T2 polypeptide, Hum. Mutat. 21 (2003) 587–592.

[18] T. Fukao, G-X Zhang, N. Sakura, T. Kubo, H. Yamaga, H. Hazama, Y. Kohno, N. Matsuo, M. Kondo, S. Yamaguchi, Y. Shigematsu, N. Kondo, The mitochondrial acetoacetyl-CoA thiolase deficiency in Japanese patients: urinary organic acid and blood acylcarnitine profiles under stable conditions have subtle abnormalities in T2-deficient patients with some residual T2 activity, J. Inherit. Metab. Dis. 26 (2003) 423–431.
[19] G.X. Zhang, T. Fukao, M.O. Rolland, M.T. Zabot, G. Renom, E. Touma, M. Kondo, N. Matsuo, N. Kondo, The mitochondrial acetoacetyl-CoA thiolase (T2) deficiency: T2-deficient patients with mild mutation(s) were previously misinterpreted as normal by the coupled assay with tiglyl-CoA, Pediatr. Res. 56 (2004) 60–64.
[20] L. Mrazova, T. Fukao, K. Halovd, E. Gregova, V. Kohut, D. Pribyl, P. Chrastina, N. Kondo, E. Pospisilova, Two novel mutations in mitochondrial acetoacetyl-CoA thiolase deficiency, J. Inherit. Metab. Dis. 28 (2005) 235–236.
[21] G.X. Zhang, T. Fukao, S. Sakurai, K. Yamada, K.M. Gibson, N. Kondo, Identification of Alu-mediated, large deletion-spanning exons 2–4 in a patient with mitochondrial acetoacetyl-CoA thiolase deficiency, Mol. Genet. Metab. 89 (2006) 222–226.
[22] S. Sakurai, T. Fukao, A.M. Haapalainen, G. Zhang, S. Yamada, F. Lilliu, S. Yano, P. Robinson, M.K. Gibson, R.J.A. Wanders, G.A. Mitchell, R.K. Wierenga, N. Kondo, Kinetic and expression analyses of seven novel mutations in mitochondrial acetoacetyl-CoA thiolase (T2): identification of a Km mutant and an analysis of the mutational sites in the structure, Mol. Genet. Metab. 90 (2007) 370–378.
[23] T. Fukao, G. Zhang, M-O. Rolland, M-T. Zabot, N. Guffon, Y. Aoki, N. Kondo, Identification of an Alu-mediated tandem duplication of exons 8 and 9 in a patient with mitochondrial acetoacetyl-CoA thiolase (T2) deficiency, Mol. Genet. Metab. 92 (2007) 375–378.
[24] T. Fukao, A. Boneh, Y. Aoki, N. Kondo, A novel single-base substitution (c.1124A>G) that activates a 5-base upstream cryptic splice donor site within exon 11 in the human mitochondrial acetoacetyl-CoA thiolase gene, Mol. Genet. Metab. 94 (2008) 417–421.
[25] S. Thümmler, D. Dupont, C. Acquaviva, T. Fukao, D. de Ricaud, Different clinical presentation in siblings with mitochondrial acetoacetyl-CoA thiolase deficiency and identification of two novel mutations, Tohoku J. Exp. Med. 220 (2010) 27–31.
[26] T. Fukao, X.Q. Song, S. Yamaguchi, T. Hashimoto, T. Orii, N. Kondo, Immunotitration analysis of cytocolic acetoacetyl-coenzyme A thiolase activity in human fibroblasts, Pediatr. Res. 39 (1996) 1055–1058.
[27] T. Fukao, X.Q. Song, G.A. Mitchell, S. Yamaguchi, K. Sukegawa, T. Orii, N. Kondo, Enzymes of ketone body utilization in human tissues: protein and mRNA levels of succinyl-CoA: 3-ketoacid CoA transferase and mitochondrial and cytosolic acetoacetyl-CoA thiolases, Pediatr. Res. 42 (1997) 498–502.
[28] H. Niwa, K. Yamamura, J. Miyazaki, Efficient selection for high-expression transfectants with a novel eukaryotic vector, Gene 108 (1991) 192–200.
[29] H. Watanabe, K.E. Orii, T. Fukao, X-Q. Song, T. Aoyama, L. IJlst, J. Ruiter, R.J.A. Wanders, N. Kondo, Molecular basis of very long chain acyl-CoA dehydrogenase deficiency in three Israeli patients: identification of a complex mutant allele with P65L and K247Q mutations, the former being an exonic mutation causing exon 3 skipping, Hum. Mutat. 15 (2000) 430–438.
[30] P.J. Smith, C. Zhang, J. Wang, S.L. Chew, M.Q. Zhang, A.R. Krainer, An increased specificity score matrix for the prediction of SF2/ASF-specific exonic splicing enhancers, Hum. Mol. Genet. 15 (2006) 2490–2508.
[31] L. Cartegni, J. Wang, Z. Zhu, M.Q. Zhang, A.R. Krainer, ESEfinder: a web resource to identify exonic splicing enhancers, Nucleic Acid Res. 31 (2003) 3568–3571.
[32] A.C. Goldstrohm, A.L. Greenleaf, M.A. Garcia-Blanco, Co-transcriptional splicing of pre-messenger RNAs: considerations for the mechanism of alternative splicing, Gene 277 (2001) 31–47.
[33] T.A. Cooper, W. Mattox, The regulation of splice-site selection, and its role in human disease, Am. J. Hum. Genet. 61 (1997) 259–266.
[34] B.L. Robbertson, G.J. Cote, S.M. Berget, Exon definition may facilitate splice site selection in RNAs with multiple exons, Mol. Cell. Biol. 10 (1990) 84–94.
[35] M.B. Shapiro, P. Senapathy, RNA splice junctions of different classes of eukaryotes: sequence statistics and functional implications in gene expression, Nucleic Acids Res. 15 (1987) 7155–7174.
[36] S. Lin, X.D. Fu, SR proteins and related factors in alternative splicing, Adv. Exp. Med. Biol. 623 (2007) 107–122.
[37] A. Boichard, L. Venet, T. Naas, A. Boutron, L. Chevret, H.O. de Baulny, P. De Lonlay, A. Legrand, P. Nordman, M. Brivet, Two silent substitutions in the PDHA1 gene cause exon 5 skipping by disruption of a putative exonic splicing enhancer, Mol. Genet. Metab. 93 (2008) 323–330.
[38] V. Gonçalves, P. Theisen, O. Antunes, A. Medeira, J.S. Ramos, P. Jordan, G. Isidro, A missense mutation in the APC tumor suppressor gene disrupts an ASF/SF2 splicing enhancer motif and causes pathogenic skipping of exon 14, Mutat. Res. 662 (2009) 33–36.
[39] P.Y. Ho, M.Z. Huang, V.T. Fwu, S.C. Lin, K.J. Hsiao, T.S. Su, Simultaneous assessment of the effects of exonic mutations on RNA splicing and protein functions, Biochem. Biophys. Res. Commun. 373 (2008) 515–520.

Clinical Immunology (2011) 138, 172–177

available at www.sciencedirect.com

Clinical Immunology

www.elsevier.com/locate/yclim

Analysis of mutations and recombination activity in RAG-deficient patients

Erika Asai[a], Taizo Wada[a,*], Yasuhisa Sakakibara[a], Akiko Toga[a], Tomoko Toma[a], Takashi Shimizu[b], Sheela Nampoothiri[c], Kohsuke Imai[d], Shigeaki Nonoyama[d], Tomohiro Morio[e], Hideki Muramatsu[f], Yoshiro Kamachi[f], Osamu Ohara[g], Akihiro Yachie[a]

[a] *Department of Pediatrics, School of Medicine, Institute of Medical, Pharmaceutical and Health Sciences, Kanazawa University, Kanazawa, Japan*
[b] *Department of Pediatrics, Tokai University School of Medicine, Isehara, Japan*
[c] *Department of Pediatric Genetics, Amrita Institute of Medical Sciences and Research Center, Cochin, India*
[d] *Department of Pediatrics, National Defense Medical College, Saitama, Japan*
[e] *Department of Pediatrics, Tokyo Medical and Dental University, Tokyo, Japan*
[f] *Department of Pediatrics, Nagoya University Graduate School of Medicine, Nagoya, Japan*
[g] *Kazusa DNA Research Institution, Chiba, Japan*

Received 27 September 2010; accepted with revision 3 November 2010
Available online 4 December 2010

KEYWORDS
RAG deficiency;
SCID;
Omenn syndrome;
TCRγδ⁺ T cells;
V(D)J recombination

Abstract Mutations in the recombination activating genes (*RAG1* or *RAG2*) can lead to a variety of immunodeficiencies. Herein, we report 5 cases of RAG deficiency from 5 families: 3 of Omenn syndrome, 1 of severe combined immunodeficiency, and 1 of combined immunodeficiency with oligoclonal TCRγδ⁺ T cells, autoimmunity and cytomegalovirus infection. The genetic defects were heterogeneous and included 6 novel *RAG* mutations. All missense mutations except for Met443Ile in *RAG2* were located in active core regions of *RAG1* or *RAG2*. V(D)J recombination activity of each mutant was variable, ranging from half of the wild type activity to none, however, a significant decrease in average recombination activity was demonstrated in each patient. The reduced recombination activity of Met443Ile in *RAG2* may suggest a crucial role of the non-core region of RAG2 in V(D)J recombination. These findings suggest that functional evaluation together with molecular analysis contributes to our broader understanding of RAG deficiency.

1. Introduction

V(D)J recombination mediated by the recombination activating genes (RAG) 1 and RAG2 leads to the generation of diverse antigen receptors [1]. A complete lack of RAG activity causes severe combined immunodeficiency (SCID) with the

* Corresponding author. Department of Pediatrics, School of Medicine, Institute of Medical, Pharmaceutical and Health Sciences, Kanazawa University, 13-1 Takaramachi, Kanazawa 920-8641, Japan. Fax: +81 76 262 1866.
E-mail address: taizo@staff.kanazawa-u.ac.jp (T. Wada).

1521-6616/$ – see front matter © 2010 Elsevier Inc. All rights reserved.
doi:10.1016/j.clim.2010.11.005

absence of mature T and B cells, but the presence of natural killer (NK) cells (T^-B^- SCID) [2], whereas partial loss results in variant syndromes, such as Omenn syndrome (OS) [3] or combined immunodeficiency (CID) presenting with oligoclonal TCR$\gamma\delta^+$ T cells, autoimmunity and cytomegalovirus (CMV) infection (CID with $\gamma\delta$/CMV) [4,5]. OS is characterized by early-onset generalized erythroderma, lymphadenopathy, hepatosplenomegaly, protracted diarrhea, failure to thrive, eosinophilia, hypogammaglobulinemia, elevated serum IgE levels, the absence of B cells, and the presence of activated and oligoclonal T cells [6]. In contrast to T^-B^- SCID and OS, patients affected with CID with $\gamma\delta$/CMV exhibit autoimmune cytopenias, B cells, normal immunogulobulin levels, oligoclonal TCR$\gamma\delta^+$ T cells, and disseminated CMV infections [4,5]. Very recently, another distinct clinical syndrome caused by hypomorphic *RAG* mutations has been described. Schuetz et al. [7] reported 3 patients with late age of onset of illness characterized by hypogammaglobulinemia, diminished numbers of T and B cells, and the formation of granulomas in the skin, mucous membranes and internal organs. De Ravin et al. [8] described an adolescent patient presenting with destructive midline granulomatous disease who also exhibited autoimmunity, relatively normal numbers of T and B cells, and a diverse T-cell receptor (TCR) repertoire.

Herein, we report the identification of 8 *RAG* mutations including 6 novel mutations in a group of patients presenting with a variety of clinical phenotypes, and discuss the functional significance of these mutations by using the V(D)J recombination assay.

2. Materials and methods

2.1. Patients

We studied five patients with RAG deficiency from five families. Table 1 presents the immunological features of the patients. All patients except for patient 5 were born to non-consanguineous Japanese parents. The clinical and immunological data of patient 1 and patient 3 have been reported elsewhere [9]. Patient 2 was a 1-month-old boy who presented with generalized erythroderma, hepatosplenomegaly and *Pseudomonas aeruginosa* sepsis. Laboratory studies revealed hypereosinophilia, hypogammaglobulinemia, lack of B cells, and oligoclonal expansion of activated TCR$\alpha\beta^+$ T-cells. These findings were consistent with typical features of OS. Patient 4 was a 2-year-old girl who presented with prolonged diarrhea, bronchopneumonia, liver dysfunction and CMV infections. CMV was detected in her stool and sputum. Laboratory analysis revealed lymphopenia with normal immunoglobulin levels, an increased percentage of TCR$\gamma\delta^+$ T cells (61.7% of $CD3^+$), and multiple autoantibodies including anti-nuclear, anti-DNA, and antiparietal cell antibodies and Coombs test. In addition, IgG antibody against CMV was detected (20.7; normal, <2.0). Her elder sister suffered from autoimmune hemolytic anemia and immune mediated thrombocytopenia, and died of fatal interstitial pneumonia of adenovirus at age of 1 year. Patient 5 was the fourth child born to non-consanguineous parents of Indian origin. All of her 3 siblings were affected with immunodeficiency and died within the first year of life. Patient 5 showed lymphopenia, very low numbers of autologous T and B cells, preserved numbers of NK cells, and the presence of maternal $CD4^+$ T cell engraftment. At the age of 2 months, she remained asymptomatic except for oral thrush and microcephaly.

Table 1 Immunological features of the patients at diagnosis.

Patient	1[a]	2	3[a]	4	5
Diagnosis	OS	OS	Atypical OS	CID with $\gamma\delta$/CMV	Atypical SCID with MFT
Age at onset (month)	0	0	7	8	0
WBC	26,900	19,000	2800	3900	3280
Lymphocytes ($/mm^3$)	8339	5700	1300	546	459
$CD3^+$ (%)	84.8	41.3	20.0	53.9	7.8
$CD4^+$ (%)	56.7	16.6	17.3	9.9	7.4
$CD8^+$ (%)	27.0	37.8	1.3	35.4	0.1
$CD19^+$ or 20^+ (%)	0.0	0.2	0.1	11.6	0.1
IgG (mg/dl)	461	220	328	678	1475
IgA (mg/dl)	<4	<1	62	63	114
IgM (mg/dl)	<4	<2	31	65	147
IgE (IU/ml)	7	<2	16	NA	NA

OS, Omenn syndrome; CID, combined immunodeficiency; $\gamma\delta$, TCR$\gamma\delta^+$ T cells; CMV, cytomegalovirus; SCID, severe combined immunodeficiency; MFT, maternal T-cell engraftment; WBC, white blood cells; NA, not available.

[a] Data of patient 1 and patient 3 have been reported previously [9].

Approval for this study was obtained from the Human Research Committee of Kanazawa University Graduate School of Medical Science, and informed consent was provided according to the Declaration of Helsinki.

2.2. Mutation analysis of RAG1 and RAG2

DNA was extracted from blood samples using standard methods. The *RAG1* and *RAG2* genes were amplified in several segments from genomic DNA using specific primers, as previously described [10,11]. Sequencing was performed on purified polymerase chain reaction (PCR) products using the ABI Prism BigDye Terminator Cycle sequencing kit on an ABI 3100 automated sequencer (Applied Biosystems, Foster, CA).

2.3. V(D)J recombination assay

In vivo V(D)J recombination assay was performed by using the recombination substrate pJH200 as described previously with modifications [3,12]. The complete open reading frames of human *RAG1* and *RAG2*, and the active core regions of mouse *RAG1* (aa 330–1042) and *RAG2* (aa 1–388) were subcloned into the mammalian expression vector pEF-BOS [13]. PCR products carrying the patients' mutations were also subcloned into the vector. Cotransfections of full-length human *RAG1*, the mouse *RAG2* active core, and pJH200, or of full-length human *RAG2*, the mouse *RAG1* active core, and pJH200 into 293T cells were performed using 1 μg of each plasmid with Lipofectamine 2000 (Invitrogen, Carlsbad, CA).

Cells were harvested after 48-hours of culture, and the recombined products of signal joints were analyzed for recombination frequency by PCR using primers RA-CR2 and RA-14 [14]. After 30 cycles, the amplified products were visualized by ethidium bromide staining, and the intensity of each band was quantified using Image J software (NIH, Bethesda, MD).

2.4. Analysis of IgE production and somatic hypermutation (SHM) in variable regions of IgM

Peripheral blood mononuclear cells were isolated and incubated with 500 ng/ml of anti-CD40 (Diaclone, Besançon, France) and 100 U/ml of recombinant interleukin-4 (IL-4; R&D Systems, Minneapolis, MN) for 12 days. IgE production in culture supernatants was determined by enzyme-linked immunosorbent assay as previously described [15,16]. The frequency and characteristics of SHM in the V_H3-23 region of IgM were studied in purified $CD19^+$ $CD27^+$ B cells as previously described [15,16].

3. Results

3.1. RAG mutations

As shown in Table 2, we found 2 missense and 1 nonsense mutations in *RAG2* and 4 missense and 1 nonsense mutations in *RAG1*. Two distinct novel *RAG2* mutations, R73H and Q278X, were demonstrated in patient 1. Patient 2 was found to be homozygous for a novel M443I mutation in *RAG2*. Patient 3 was a compound heterozygote bearing R142X and R396H mutations in *RAG1*. The latter mutation has been repeatedly reported in OS patients [17]. Patient 4 was a compound heterozygote bearing R474C and L732P mutations in *RAG1*. These missense mutations are novel, although similar missense mutations, R474S, R474H and L732F, have been reported in patients with RAG deficiency [17–19]. Patient 5 carried a homozygotic novel E770K mutation in *RAG1*. All missense mutations but one (M443I in *RAG2*) were located in the active core regions of *RAG1* or *RAG2*, and all patients had at least one missense mutation. None of these mutations were found in 100 alleles of healthy controls.

Table 2 *RAG* mutations and recombination activity.

Patient	Gene	Nucleotide mutation	Effect	Relative recombination activity (%) [a]
1	RAG2	1419 G>A	R73H	59.3±4.7
		2033 C>T	Q278X	0.4±0.3
2	RAG2	2530 G>T [b]	M443I	8.7±1.2
3	RAG1	536 C>T	R142X	51.2±9.2
		1299 G>A	R396H	1.0±0.5
4	RAG1	1532 C>T	R474C	47.2±7.9
		2307 T>C	L732P	0.5±0.4
5	RAG1	2420 G>A [b]	E770K	15.6±9.1
Control	RAG2	wild type	–	100
	RAG1	wild type	–	100

[a] Data are expressed as the percentage of activity as compared with that of the wild type protein, and represent the mean±standard deviation of three independent experiments.
[b] Homozygous mutation.

3.2. Recombination activity of RAG mutants

To elucidate the pathogenic significance of these novel mutations, we performed V(D)J recombination assay using the artificial extrachromosomal rearrangement substrate (Table 2). As expected, the recombined products were amplified from 293T cells transfected with both wild type RAG1 and RAG2, and no products were obtained from 293T cells transfected with either RAG1 or RAG2 (Fig. 1). Although the relative recombination activity of each mutant was variable, ranging from about half of the wild type activity to none, a significant decrease in average recombination activity was demonstrated in each patient (Fig. 1 and Table 2). The effects of the patients' missense mutations were also evaluated by the web-based analysis tools including Mutation@A Glance (http://rapid.rcai.riken.jp/mutation/) [20] and MutationTaster (http://www.mutationtaster.org/) [21]. Mutation@A Glance predicted all the mutation except for the E770K in *RAG1* to be deleterious on the basis of the SIFT program [22], whereas MutationTaster predicted all the missense mutations to be disease-causing.

3.3. B cell analysis of patient 4

The percentages of IgD^- $CD27^+$ and IgD^+ $CD27^+$ cells within $CD19^+$ B cells from patient 4 were found comparable to controls (Fig. 2A) [23]. After stimulation with anti-CD40 and IL-4, B cells from patient 4 produced levels of IgE equivalent to normal, indicating their capability of undergoing class

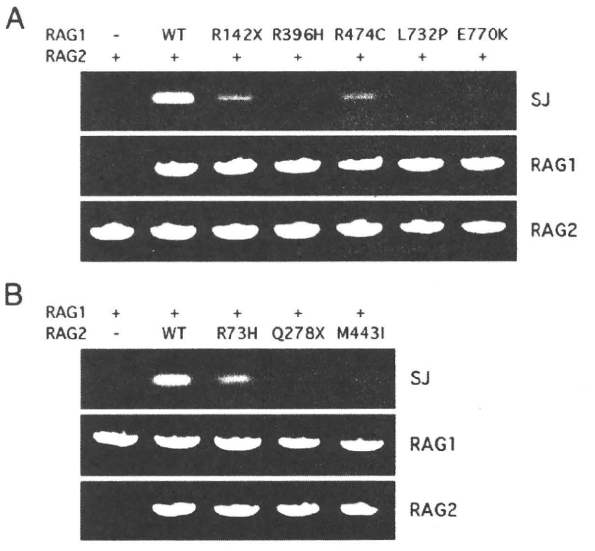

Figure 1 V(D)J recombination assay. V(D)J recombination activity was assessed by using the recombination substrate pJH200 in 293T cells that were cotransfected with mutant RAG1 and wild type RAG2 (A), or with wild type RAG1 and mutant RAG2 (B). Recombined products (signal joints, SJ) were analyzed by PCR (top). The presence of RAG1 and RAG2 was verified by vector specific PCR (middle and bottom).

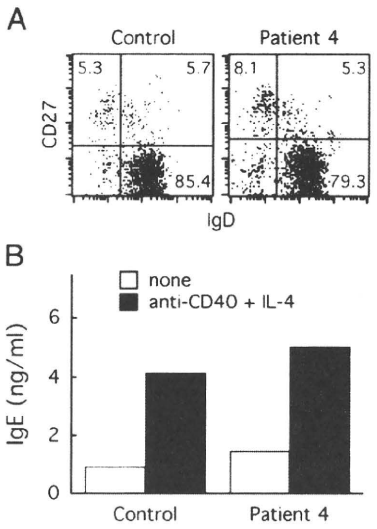

C

%	Patient 4	Controls
SHM	4.8	2.6-6.3
GC target	56.0	62-66
GC transition	71.4	57-63
AT transition	50.0	33-67

To

From %	A	C	G	T	Total
A		5	13	10	28
C	2		6	11	19
G	29	6		2	37
T	2	9	5		16

Patient 4

From %	A	C	G	T	Total
A		6.2	12.9	4.1	23.2
C	2.6		6.0	11.4	20.0
G	26.1	13.2		4.3	43.6
T	4.8	5.5	3.0		13.2

Control

Figure 2 B cell analysis of patient 4. (A) B cell subpopulations. Peripheral bloods were stained with FITC-labeled anti-IgD, PE-labeled anti-CD27, and APC-labeled anti-CD19 monoclonal antibodies. The dot plot of immunofluorescence profiles of IgD and CD27 expression within $CD19^+$ B cells is shown. The number indicates the percentage of cells in each quadrant. (B) IgE production. After stimulation of peripheral blood mononuclear cells with anti-CD40 and IL-4 for 12 days, concentrations of IgE in the culture medium were quantified. (C) The frequency and pattern of somatic hypermutation in the V_H3-23 region of the IgM in memory B cells. RT-PCR products amplified from purified $CD19^+$ $CD27^+$ B cells by using V_H3-23 and $C\mu$ primers were subcloned and sequenced. Nucleotide changes were evaluated and shown as percentages.

switch recombination and IgE synthesis *in vitro* (Fig. 2B). In addition, the frequency and nucleotide substitution patterns of SHM were similar to those of healthy individuals (Fig. 2C).

4. Discussion

RAG deficiency has been considered to display a range of phenotype from classical T^-B^- SCID (complete RAG deficiency) to OS (partial RAG deficiency), depending on residual V(D)J recombination activity [24]. Atypical SCID/OS or leaky SCID may be also diagnosed in patients who show incomplete clinical and immunological characteristics and do not fulfill the criteria for SCID or OS [17]. However, it has recently been recognized that the clinical spectrum of RAG deficiency is much broader and includes CID with γδ/CMV [4,5], and CID with granulomatous inflammation [7], or destructive midline granulomatous disease [8]. In the present study, we studied 5 cases of RAG deficiency including 3 of OS, 1 of CID with γδ/CMV, and 1 of SCID with maternal T-cell engraftment, and identified 6 novel and 2 recurrent *RAG* mutations in these patients.

Hypomorphic RAG mutations leading to immunodeficiency have been shown to have up to 30% of wild type RAG activity by V(D)J recombination assay [7]. Although the R73H mutation in *RAG2* from patient 1, the R142X mutation in *RAG1* from patient 3, and the R474C mutation in *RAG1* from patient 4 exhibited around half of the wild type activity, all of these patients also had mutations with extremely low levels of recombination activity on the other allele, resulting in a substantial decrease in the average recombination activity due to a tetrameric complex formation of RAG1 and RAG2 during V(D)J recombination [1]. Similar results were obtained from an investigation of a RAG-deficient patient with destructive granulomatous disease who carried a W522C mutation with half of the recombination activity and a L541CfsX30 mutation with no recombination activity in *RAG1* [8]. It therefore seems reasonable that the clinical phenotype of partial RAG deficiency in patients 1, 3 and 4 is a consequence of these combinations of the mutations.

Biochemical studies have identified the core regions of RAG1 and RAG2 that are the minimal regions necessary for recombination of exogenous plasmid substrates *in vivo* and for DNA cleavage *in vitro* [1]. The M443I missense mutation demonstrated in patient 2 was located in the noncanonical plant homeodomain (PHD) of the non-core region of RAG2. Recent evidence indicates the importance of the non-core regions of RAG1 and RAG2 in V(D)J recombination and lymphocyte development [25]. The PHD of RAG2 has been shown to play crucial roles for chromatin and phosphoinositide binding, regulation of protein turnover, and cellular localization of RAG2 [26]. Additionally, the PHD of RAG2 is known to recognize histone H3 that has been trimethylated at the lysine at position 4 by interacting with 4 essential amino acids, Y415, M443, Y445, and W453 [27]. To date, 8 mutations of the non-core region in *RAG2* (W416L, K440N, W453R, A456T, C446W, N474S, C478Y, and H481P) have been reported in patients with T^-B^- SCID or OS [28]. A significant decrease in recombination activity of the M443I mutation from our patient further supports the important role of PHD of RAG2 in regulating V(D)J recombination.

Although the R142X nonsense mutation found in the N-terminal domain of RAG1 in patient 3 should have resulted in a complete loss of function, it remained partially functional for recombination unlike the Q278X mutation in RAG2 in our assay. On the other hand, the same R142X mutation has been described in a typical OS patient who also had a nonfunctional frameshift mutation in the core region of RAG1 on the other allele, thus suggesting that the residual V(D)J recombination activity exists